

RESEARCH ARTICLE

Strong correlations of sea ice cover with macroalgal cover along the Antarctic Peninsula: Ramifications for present and future benthic communities

Charles D. Amsler^{1,*†} , Margaret O. Amsler^{1,†}, Andrew G. Klein^{2,‡}, Aaron W. E. Galloway³, Katrin Iken⁴, James B. McClintock¹, Sabrina Heiser^{1,5}, Alex T. Lowe⁶, Julie B. Schram^{3,7}, and Ross Whippo³

Macroalgal forests dominate shallow hard bottom areas along the northern portion of the Western Antarctic Peninsula (WAP). Macroalgal biomass and diversity are known to be dramatically lower in the southern WAP and at similar latitudes around Antarctica, but few reports detail the distributions of macroalgae or associated macroinvertebrates in the central WAP. We used satellite imagery to identify 14 sites differing in sea ice coverage but similar in terms of turbidity along the central WAP. Fleshy macroalgal cover was strongly, negatively correlated with ice concentration, but there was no significant correlation between macroinvertebrate cover and sea ice. Overall community (all organisms) diversity correlated negatively with sea ice concentration and positively with fleshy macroalgal cover, which ranged from around zero at high ice sites to 80% at the lowest ice sites. Nonparametric, multivariate analyses resulted in clustering of macroalgal assemblages across most of the northern sites of the study area, although they differed greatly with respect to macroalgal percent cover and diversity. Analyses of the overall communities resulted in three site clusters corresponding to high, medium, and low fleshy macroalgal cover. At most northern sites, macroalgal cover was similar across depths, but macroalgal and macroinvertebrate distributions suggested increasing effects of ice scour in shallower depths towards the south. Hindcast projections based on correlations of ice and macroalgal cover data suggest that macroalgal cover at many sites could have been varying substantially over the past 40 years. Similarly, based on predicted likely sea ice decreases by 2100, projected increases in macroalgal cover at sites that currently have high ice cover and low macroalgal cover are substantial, often with only a future 15% decrease in sea ice. Such changes would have important ramifications to future benthic communities and to understanding how Antarctic macroalgae may contribute to future blue carbon sequestration.

Keywords: Benthic ecology, Climate change, Depth distribution, Ice scour, Polar ecosystems, Sea ice

¹Department of Biology, University of Alabama at Birmingham, Birmingham, AL, USA

²Department of Geography, Texas A&M University, College Station, TX, USA

³Oregon Institute of Marine Biology, Department of Biology, University of Oregon, Charleston, OR, USA

⁴College of Fisheries and Ocean Sciences, University of Alaska Fairbanks, Fairbanks, AK, USA

⁵Current address: Marine Science Institute, University of Texas at Austin, Port Aransas, TX, USA

⁶Tennenbaum Marine Observatories Network, Smithsonian Institution, Edgewater, MD, USA

⁷Current address: Department of Natural Science, University of Alaska Southeast, Juneau, AK, USA

*Corresponding author:
Email: amsler@uab.edu

†Joint first authors

‡Lead co-author

1. Introduction

Globally, the growth and productivity of photoautotrophs can be limited by light, nutrients, temperature, or, in terrestrial environments, the availability of water (Field et al., 1998). Although marine microalgae and macroalgae are commonly growth-limited by nutrients (Falkowski and Raven, 2007; Hurd et al., 2014), Antarctic macroalgae are limited primarily by light (Wiencke et al., 2007; Deregibus et al., 2020). Light availability to the Antarctic benthos is impacted by shading from phytoplankton blooms, sediment runoff from melting glacial ice, and particularly by overlying sea ice (Knox, 2007; Deregibus et al., 2020; Huovinen and Gómez, 2020).

Annual sea ice extent in the Southern Ocean surrounding Antarctica as a whole has varied dramatically over recent years (Stammerjohn and Maksym, 2017; Maksym, 2019; Eays et al., 2021), including record high extent in 2014 and record low extent in 2017 (Eays et al., 2021).

Although the sea ice cover around the continent as a whole increased between 1979 and 2014, the Bellinghshausen/Amundsen Sea region, which includes the Western Antarctic Peninsula (WAP; **Figure 1**), experienced an overall decline in ice cover (Stammerjohn and Maksym, 2017). Mean sea ice cover along the WAP substantially decreased during the second half of the 20th century,

which was consistent with observed warming in the region (Ducklow et al., 2007; Turner et al., 2016). Although air temperatures have cooled slightly since 1999 and sea ice cover off the northernmost portion of the WAP region increased (Turner et al., 2016), sea ice cover has not increased significantly over the central portion of the WAP, at least until recently (Obryk et al., 2016;

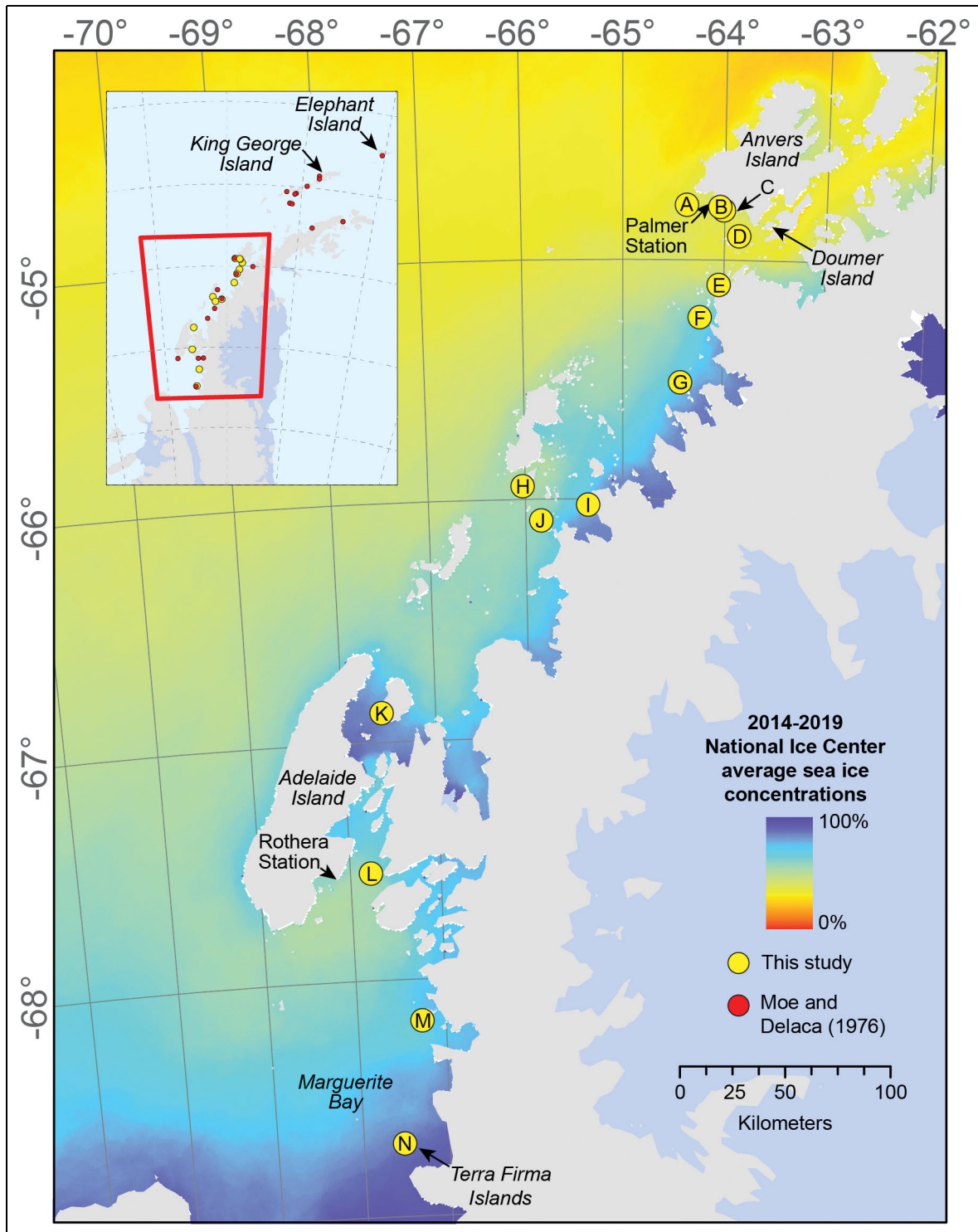


Figure 1. Study sites along the central Western Antarctic Peninsula. Inset shows the entire Antarctic Peninsula, with both our sites and those of Moe and Delaca (1976) indicated along the western side of the Peninsula. The 14 research sites, designated north to south as A through N, were studied between April 23 and May 18, 2019. Their locations spanned the range of annual sea ice coverage (color scale bar); coordinates are provided in Table S1.

Turner et al., 2016; Henley et al., 2019). These changes in annual sea ice cover along the WAP have had notable impacts on marine ecosystems (Clarke et al., 2007; Ducklow et al., 2007; Ducklow et al., 2013; Kerr et al., 2018; Henley et al., 2019; Lin et al., 2021). A majority of these previous studies of the influence of annual sea ice cover on WAP marine ecosystems have focused on pelagic communities, although the influence of annual sea ice cover on the structure of deep water, soft substrate benthic communities has also received some attention (Smith et al., 2012; Säring et al., 2022).

Macroalgae dominate shallow benthic communities on hard substrates along the northern portion of the WAP, often covering over 80% of the bottom and with standing biomass levels comparable to temperate kelp forests (Wiencke and Amsler, 2012; Quartino et al., 2020). Recent modeling has predicted that the net primary production of subtidal macroalgae on the WAP and in many other polar areas exceeds that of coastal phytoplankton by 10-fold (Pessarrodona et al., 2022), although only a few empirical studies of WAP macroalgal productivity were available to the authors. Several species of large, perennial brown algae are particularly abundant along the WAP. *Desmarestia menziesii* and/or *Desmarestia anceps* typically dominate in shallower waters down to approximately 10–20 m depth with *Himantothallus grandifolius* dominating from 10–20 m down to 40 m or greater (Wiencke and Amsler, 2012; Wiencke et al., 2014). *Cystosphaera jacquinotii* can co-dominate with *H. grandifolius* below 25 m, and *Ascoseira mirabilis* or *Desmarestia antarctica* can sometimes be locally important in shallower waters (Wiencke et al., 2014). Although these species dominate in biomass, well over 100 species of macroalgae are found in shallow water along the WAP (Wiencke and Amsler, 2012; Wiencke et al., 2014; Oliveira et al., 2020).

This general pattern of macroalgal dominance has been reported since 1906 including at least 38 times since 1965 (Appendix S1) from numerous locations along the broader WAP region from its northeastern limit at Signy Island (60°S) south to Anvers Island (64°S; **Figure 1**). However, we are aware of only limited qualitative reports and of no quantitative data on the relative abundance or importance of macroalgae and other hard-bottom biota farther south between Anvers Island and Adelaide Island (67.6°S; **Figure 1**). In the early 1970s, Moe and DeLaca (1976) and DeLaca and Lipps (1976) visited 32 sites along the WAP between Elephant Island (61.2°S) and the Terra Firma Islands in Marguerite Bay (68.7°S), including 14 sites south of Anvers Island (**Figure 1**). Both qualitative reports describe a drop off in both species richness and biomass south of Anvers Island. These reports also qualitatively describe decreases in richness and biomass at more turbid, protected sites compared with exposed sites. Among the major biomass contributors, only *Desmarestia menziesii* and *Himantothallus grandifolius* were reported as far south as Adelaide Island (**Figure 1**). None of the other common brown algae were reported farther south than 66°S. These records correspond with more recent qualitative and quantitative studies near Rothera Station (**Figure 1**) on Adelaide Island (Barnes and Brockington, 2003;

Bowden, 2005; Mystikou et al., 2014). Relatively low species richness is also described from other locations of similar latitude throughout Antarctica (e.g., Zaneveld, 1966; Dhargalkar et al., 1988; Kirkwood and Burton, 1988; Irving et al., 2005; Johnston et al., 2007; Clark et al., 2013; Clark et al., 2015a), although cover of the relatively few macroalgal species can be substantial at some sites, at least over narrow depth ranges (e.g., Irving et al., 2005; Johnston et al., 2007).

Moe and DeLaca (1976) hypothesized that the observed decreases in macroalgal biomass and diversity in more southerly sites along the WAP were the result of decreased light levels caused by increasing annual sea ice cover. This is consistent with a strong inverse correlation between annual sea ice cover and macroalgal abundance in bays in the Windmill Islands (66°S in East Antarctica) reported by Clark et al. (2013). They also measured the underwater light levels at their sites along with the light requirements for growth in the four dominant macroalgae (*Desmarestia menziesii*, *Himantothallus grandifolius*, and two smaller red macroalgae). Using those data, they modeled the impact of increased irradiance due to reduced sea ice cover and predicted that even relatively modest decreases in ice cover could result in sites currently dominated by benthic macroinvertebrates switching to dominance by fleshy macroalgae (Clark et al., 2013). Subsequent modeling suggested that the same pattern was likely in other parts of Antarctica (Clark et al., 2015b). The corresponding situation with increasing changes in ice cover has been observed at another site in East Antarctica, Commonwealth Bay (67°S), which historically was ice-free most of the year due to strong winds except where annual sea ice coverage became continuous because of the grounding of a huge iceberg in 2010 (Clark et al., 2015a). Within 3 years of the grounding, the macroalgae were either decomposing or at least severely bleached, while benthic invertebrates were increasing in abundance (Clark et al., 2015a).

Macroalgae along the WAP contribute to the base of the food web (Dunton, 2001; Aumack et al., 2017). However, most abundant Antarctic macroalgal species are chemically defended from herbivores and probably are rarely consumed while alive (Amsler et al., 2014, 2020). A single amphipod species, *Paradexamine fissicauda*, is known to be able to consume a few chemically defended red macroalgae, including the relatively widespread species *Plocamium* sp. and *Picconiella plumosa* (Amsler et al., 2013; Heiser et al., 2020). *Palmaria decipiens*, which can be locally abundant, is the only common species known to be palatable to a variety of herbivores (Becker et al., 2011; Amsler et al., 2020). However, the widespread overstory brown macroalgae *Himantothallus grandifolius* (Reichardt and Dieckmann, 1985) and *Desmarestia anceps* (Amsler et al., 2012a; Braeckman et al., 2019) become relatively palatable to amphipods and other consumers within weeks of death. Carbon from other chemically defended macroalgae are probably also important contributors to local consumers based on analyses of stable isotopes, fatty acids, and gut contents of macroalgal-associated amphipods (Aumack et al., 2017).

Macroalgal carbon is of particular importance to Antarctic benthic detrital food chains (Dunton, 2001; Corbier et al., 2004; Quartino et al., 2008). Benthic detrital food chains based on macroalgae should be much less seasonal than those based on phytoplankton blooms, and thus macroalgae may be much more important as a carbon source for the Antarctic benthos than they are in temperate seas (Reichardt, 1987). Drift macroalgae are abundant in pockets on the coastal seafloor (Neushul, 1965; Brouwer, 1996a; C Amsler, M Amsler, K Iken, personal observations). Macroalgae are one of the major sources of dissolved and particulate detritus in coastal waters (Dawson et al., 1985; Lastra et al., 2014). Macroalgal fragments can be common even in deep-water Antarctic communities (Reichardt, 1987; Fischer and Wiencke, 1992; Grange and Smith, 2013; M Amsler, personal observations), and biogenic flux and stable carbon isotope studies have suggested that macroalgae can be major sources of deep-water sediment carbon (Liebezeit and von Bogungen, 1987; Fischer and Wiencke, 1992). The kinetics of macroalgal detritus formation is as efficient in the Antarctic as in lower latitudes (Reichardt and Dieckmann, 1985), and Antarctic sedimentary bacterial communities actively degrade macroalgal detritus (Aromokeye et al., 2021). A major portion of the primary production of *Himantothalpus grandifolius* is lost by blade erosion; in contrast to phytoplankton, this carbon input to the detrital communities continues throughout the year (Dieckmann et al., 1985). Although living drift *Desmarestia anceps* decays fairly slowly via fragmentation, carbon from dead macroalgae is recycled relatively quickly (mostly within 90 days or less; Brouwer, 1996a; Braeckman et al., 2019). In shallow, soft bottom communities macroalgal fragments form an important nutritional component of diets for several animal groups including amphipods, ascidians, sea urchins, fish, sea cucumbers, bivalves, and polychaetes (Corbier et al., 2004; Tatián et al., 2004; Tatián et al., 2008). The importance of large brown macroalgae as a carbon source in northern parts of the WAP is not surprising considering that detritus from large brown algae has been shown to be an important carbon source to shallow water communities in the sub-Antarctic (Kaehler et al., 2006; Andrade et al., 2016), Arctic (Renaud et al., 2015; Buchholz and Wiencke, 2016; Schimani et al., 2022), and many temperate regions (e.g., Duggins et al., 1989; Filbee-Dexter and Scheibling, 2014; Lowe et al., 2014).

Macroalgal-derived carbon is increasingly recognized beyond its roles in food webs, including as a potential major contributor globally to blue carbon sequestration in the context of climate change mitigation (Raven, 2018; Ortega et al., 2019; Queirós et al., 2019; Dolliver and O'Connor, 2022). Antarctica is already an important contributor to global blue carbon sequestration and is likely to become even more so as climate change increases the potential for sequestration in the Southern Ocean and diminishes the potential for sequestration elsewhere (Gogarty et al., 2019; Barnes et al., 2021; Bax et al., 2021). The increases in Antarctic blue carbon sequestration potential will come from a variety of sources, including glacial retreat uncovering new benthic habitat along

shorelines and ice shelf breakup uncovering sometimes vast areas of primarily deeper benthos, but predominantly from decreases in annual sea ice coverage that increases primary productivity (Barnes et al., 2018; Barnes et al., 2021). Most studies of blue carbon in Antarctica have not considered macroalgae, but their inclusion in blue carbon estimates for shallow waters greatly increases overall projected carbon sequestration (Morley et al., 2022). A variety of models predict that annual sea ice cover off the Antarctic continent as a whole will decline 15%–50% or more by 2100 (Cavanagh et al., 2017; Roach et al., 2020; Rackow et al., 2022). Understanding how this decline will impact macroalgal communities will be critical for Antarctic blue carbon projections.

Somewhere between the rich macroalgal communities found at Anvers Island and northward and the relatively sparse macroalgal communities found at Adelaide Island and southward, this important resource for benthic consumers becomes greatly diminished. The central hypothesis of the research reported here was that a gradient in annual sea ice coverage, primarily reflected by a latitudinal gradient, is a major driver of this geographic pattern. A main goal was to understand where and why changes in macroalgal cover occur in order to better enable understandings of the ramifications to higher trophic levels. A second goal was to understand how macroalgal cover and biomass may have been changing as annual sea ice coverage has varied in the past, and to make predictions about how ice coverage might change in the future under predicted declines in sea ice coverage due to climate change. Such changes would have ramifications not only to future benthic communities along the WAP, but also to understanding how macroalgae may contribute to future blue carbon sequestration and, therefore, the potential for increasing negative feedbacks on climate change from the shallow WAP benthos.

2. Methods

2.1. Study sites

Forty-one potential study sites between the Rosenthal Islands off the southwest coast of Anvers Island (64.6°S, 64.3°W; **Figure 1**) in the north and the Terra Firma Islands in Marguerite Bay (68.7°S, 67.5°W; **Figure 1**) in the south were identified based on the true color 15 m Pansharpended Landsat Image Mosaic of Antarctica (LIMA; Bindschadler et al., 2008). Turbidity during open water periods from 2012 to 2018 measured as a diffuse attenuation coefficient was determined using the Visible Infrared Imaging Radiometer Suite (VIIRS) Kd(490) product (Wang et al., 2017). This NOAA CoastWatch/OceanWatch program product, which estimates diffuse attenuation coefficients at 490 nm wavelength, was produced for approximately 4 × 4 km cells. To reduce potential variability in macroalgal cover due to differences in water clarity, during initial screening the only sites considered were those with January through March seasonal mean diffuse attenuation coefficients <0.1 m⁻¹ determined at 10 km spatial resolution. When the final sites were known post-cruise, diffuse attenuation coefficients in 1 × 1 km cells were calculated for January through March and,

where observations at the sites were available, during October through December. This approach resulted in some January through March seasonal means exceeding 0.1 m^{-1} (Table S1).

The potential sites were selected to encompass a range of sea ice conditions, which for initial site selection was based on the annual mean sea ice concentrations from the weekly National Ice Center Ice Charts from 2015 to 2018, which ranged from 30%–40% to 90%–100% (post-cruise analyses used 2014–2019 data from all sea ice datasets; see below for more detail). Sites were also selected in areas not directly adjacent to glacier faces based on analysis of the Landsat images. High resolution approximate 1 m satellite images from the Maxar constellation (Quickbird, Geoeye, Worldview 1, 2 and 3) of the potential study sites were obtained from the Polar Geospatial Center at the University of Minnesota and guided site selection in the field. Consequently, two potential sites were eliminated because of their proximity to shoreline glaciers, as U.S. Antarctic Program safety rules prohibit boating within 300 m of active glacier faces. From the remaining potential sites, 14 (Figure 1; Table S1) from throughout the geographic range and spanning the complete range of annual mean sea ice coverage were chosen for study between April 23 and May 18, 2019, with site selection also based on accessibility (current weather and sea ice conditions) and ship logistical constraints. The sites were designated north to south as A through N (Figure 1; Table S1).

We traveled to the vicinity of each selected site aboard the Antarctic Research and Support Vessel *Laurence M. Gould*. Prior to survey dives, we used small Zodiac boats to perform cursory benthic topography surveys using a hull-mounted Garmin EcoMap plus 74SV depth sounder or, if heavy brash ice was present, a handheld Vexilar LPS-1 depth sounder. Selection criteria were: 1) that the topography did not include substantial vertical sections, as we know from numerous research dives in the Anvers Island area that macroalgae are often underrepresented and sessile invertebrates are often overrepresented at depths of approximately 30 m and greater on vertical walls when compared to more gently sloping seafloors; 2) that depths of at least 20 m and ideally 40 m were close enough to the shore that a dive team could complete a video transect up to 5 m depth in a single dive; and 3) that these habitat characteristics spanned a great enough area for three replicate transects spaced 100 m apart to be surveyed (Figure 2). We adjusted the exact location of the central vertical transect from the location of the a priori target coordinates (before beginning dives) to allow these criteria to be met.

2.2. Video transects and collections of organisms

Video recordings at 4K resolution were made using Paralenz DC+ underwater cameras and two Light and Motion Sola 3800 video lights attached to Backscatter Double Handle GoPro and Compact Trays (Figure S1). Also attached to each tray was a custom-built mount for two Z-Bolt SCUBA-BL low temperature blue laser pointers. The mounts were carefully machined and adjusted such that

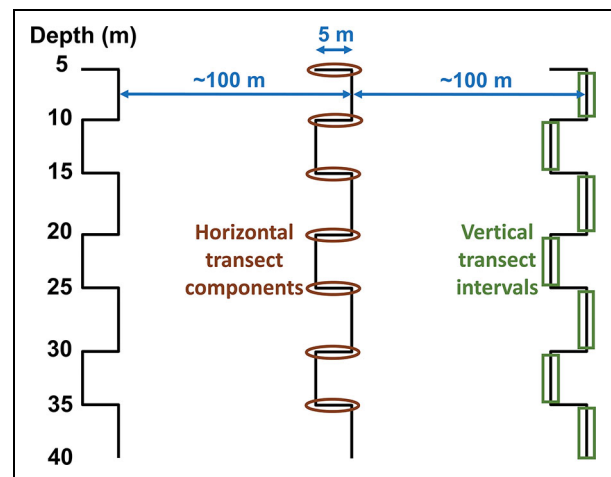


Figure 2. Design of the video transects. Analyses were made of the overall transects, the horizontal transect components separated by 5 m depths, and the vertical transect intervals that were between the horizontal components.

the two laser beams were parallel, and that the dots represented 10 cm distance on the seafloor in recordings.

Video transects began at 40 m depth wherever bottom topography allowed or at the depth where the bottom topography flattened, making it impractical to reach greater depths. The 40 m maximum depth limit was imposed by the operational requirement that all scuba dives be within no-decompression limits. One dive team member swam ahead of the camera operator and laid out a 5 m tape measure horizontally along the bottom at 5 m depth intervals beginning (where possible) at the 35 m isobath and ending at the 5 m isobath (Figure 2). The camera operator ascended along the bottom between the horizontal components and along each of the horizontal components as illustrated in Figure 2. While the camera operator swam along the horizontal components, the other diver followed and collected one of each macroalgal species they observed for later identification, placing them in individual marked bags for each of the seven 5 m depth intervals in each transect. This protocol was repeated by three dive teams, one per each of three transects. Handheld GPS units (Garmin GPSMAP 78) were used to space transects 100 m horizontally along the shore. Subsequently, an additional dive was made in the vicinity of the middle transect collecting one or more of each macroalgal species observed at any depth for later identification along with invertebrates to be used (along with macroalgae) in food web tracer studies, which will be published separately. A fifth dive focused on non-quantitative collections of smaller invertebrates associated with the substrate using an airlift device (modified from Benson, 1989) for the food web tracer studies. Some invertebrates collected by hand and via airlift are included in presence-absence data from sites if the taxon was also represented in the video data; otherwise, they were not included in analyses of the invertebrate assemblage. At one site (I on Figure 1) a ship logistical issue prevented the third transect dive and

subsequent collecting dives. At two sites (sites H and K on **Figure 1**) camera malfunctions resulted in loss of one video transect but not of other collections. At another site (G on **Figure 1**) a video backup error resulted in loss of part (5–12 m) of one transect, and a dive logistical issue resulted in the loss of the 5 m horizontal component of a second transect at that site.

Macroalgae collected from the transects and general collections were identified to the lowest possible taxonomic level (species with few exceptions) upon their return to the research ship. At least one pressed voucher specimen of each species at each site was prepared, and some species were also dried in silica gel to enable subsequent molecular sequencing, if required. Upon return to the United States, the voucher material was compared to previously identified herbarium specimens and to each other across sites to confirm identifications and ensure consistency of identifications across the study sites. Voucher material is maintained in and available from the herbarium of C.D. Amsler at the University of Alabama at Birmingham, where vouchers of species of macroinvertebrates and mesoinvertebrates from the general and airlift collections selected to be used in food web tracer studies are also maintained.

2.3. Video analyses

Video stream processing of transects was accomplished with VLC software (VideoLAN Organization) using the video scene filter set at a recording ratio of 3 frames per second. The resulting images were sized by default (–1 width, –1 height) and saved as jpg in files assigned a unique filename prefix. The first sharp image from each discrete 1 m depth interval of the vertical transect intervals (**Figure 2**) was selected for analysis. For the horizontal transect components (**Figure 2**), three to five non-overlapping images were selected. Analyses of entire transects combined the vertical intervals and horizontal components.

The selected images were loaded into Coral Point Count with Excel extensions (CPCe 4.1; National Coral Reef Institute at Nova Southeastern University; Kohler and Gill, 2006). Image scaling was calibrated based on the distance (10 cm) between the paired laser points. A grid of appropriate size was specified (<100 × 100 cm) within which fifty points were randomly overlaid. Objects (biotic and abiotic, e.g., sediment, bare rock) beneath each point were identified to the lowest taxon or category possible (Table S2) and assigned the appropriate data code. Following requirements, major categories, sub-categories and substrate categories were coded to project needs and based on species noted in voucher collections. In total the dataset included 107,000 random points from 2,140 individual images.

Data were compiled using the automatic Excel spreadsheet generation feature of CPCe (Kohler and Gill, 2006). The output for an individual screen capture summed the coded entries for each of the 50 randomly distributed points. Multiple screen captures (up to 99) could similarly be batch-processed, thus assembling an entire transect into a single unique dataset with output, including total

points in transect and number of points for each species. Post-processing included inserting columns with site, transect and depth identifiers for each individual screen capture to sort the data as desired for analyses.

To determine the overall relative percent cover of individual organisms all points for a particular taxon, either within site, transect, or depth depending on the specific analysis, were summed and divided by the corresponding total number of points. Similarly, algal points were summed at group level to determine the percent cover of fleshy green, red, and brown macroalgae. To estimate the actual percent cover of macroinvertebrates for analyses focused only on macroinvertebrates (i.e., not total community analyses), the total number of brown overstory macroalgal points was subtracted from the total number of points before determining percent cover in a site, transect, or depth. These data are referred herein to as “without overstory.” Macroinvertebrate points without overstory were summed at group level to determine the overall percent cover of sponges, echinoderms, mollusks, ascidians, and bryozoans as well as an “other” category for all other macroinvertebrate taxa. Similarly, to investigate percent cover of encrusting red macroalgal forms (crustose corallines and uncalcified red algae including *Hildenbrandia* sp. and possibly *Gania mollis*) only points that were not on larger organisms were used, excluding points that appeared to be on sediment. Percent cover of bare (without macroorganisms) space was also investigated using the same without overstory procedure as in macroinvertebrate analysis with the substrate recorded as either unambiguously bare rock or rock that appeared to have overlying sediment.

2.4. Sea ice cover determinations

Estimates of sea ice concentrations were drawn from the widely used daily Sea Ice Index (Fetterer et al., 2017), weekly National Ice Center Charts, and passive microwave sea ice concentrations from AMSR2 (Meier et al., 2018). The Sea Ice Index products are derived from Near-Real-Time DMSP SSMIS Daily Polar Gridded Sea Ice concentrations and concentrations from Nimbus-7 SMMR and DMSP SSM/I-SSMIS Passive Microwave instruments. The Sea Ice Index record extends from November 1978 to present and is available as daily raster-gridded files at 25 km resolution from the National Snow and Ice Data Center. Passive Microwave-derived AMSR2 concentrations from July 2, 2012, to present from the National Snow and Ice Data Center at 12.5 km resolution (Meier et al., 2018) were also used in the analysis. For AMSR2, daily sea ice concentrations, derived using both the NASA Team 2 (NT2) and Bootstrap algorithms, were investigated.

The weekly National Ice Center charts are produced by visual analysis of Synthetic Aperture Radar (SAR) and optical images (Dedrick et al., 2001; Fetterer, 2006). An automated procedure was used to rasterize the total ice concentration (in tenths) from the original vector GIS polygons (Esri Shapefiles) into raster grids at 1 km resolution in a WGS 1984 Stereographic South Pole Projection. All available weekly hemispherical products from 2008 to 2019 were included in the processing, which was

accomplished in Python using the Esri ArcPy package (from ArcGIS Pro 2.X). From the gridded daily Sea Ice Index or weekly National Ice Center charts, time series from the nearest grid cell to each sampling site were extracted. These point observations were then averaged into annual or summer (October–February) means for 5-year intervals ending April 1, 2019, which corresponds to the beginning of our sampling period (Table S1). Consequently, eight different ice cover datasets, both annual and summer-only for each of the four satellite data products, were used for comparison to organismal percent cover data because we had no a priori reason to believe that any of the individual datasets would be best at predicting organismal patterns.

2.5. Statistical analyses

Univariate statistical analyses were performed using SPSS v. 28 (IBM SPSS Statistics). For comparisons between sites, percent cover data were initially transformed by arcsin (square-root) as recommended by Zar (1984). If the arcsin-transformed data did not meet the assumptions of parametric statistics in either the Shapiro-Wilk or Levine's tests, the original percent cover data were transformed by ranks using SPSS and reexamined. Data transformed with either arcsin or ranks that met parametric test assumptions were analyzed using the General Linear Models (GLM) procedure with post hoc comparisons, when indicated, using the Tukey HSD test. Data that could not be transformed to satisfy the assumptions of parametric statistics were analyzed with the nonparametric Kruskal-Wallis H test. Post hoc comparisons, when indicated, were performed using pairwise Mann-Whitney U tests for categories that had at least three replicates as the test cannot distinguish significant differences for sample sizes less than three. Our conclusions are based on test results that were not corrected for type I error (Moran, 2003; Nakagawa, 2004). However, type I error corrections with the Sequential Dunn-Sidak Method (Sokal and Rohlf, 1995) were performed and are also reported where such pairwise comparisons were needed.

Overall assemblage data based on percent cover were expressed as species richness (total number of species; S) and Shannon diversity index ($H' = -\sum_i p_i \log_e(p_i)$; p_i is the proportion of the total count). Bivariate Pearson (r) correlations comparing percent cover of organism groups with the individual sea ice datasets, comparing percent covers of different organism groups, and comparing both fleshy macroalgal cover and sea ice cover with both Shannon diversity and species richness, were examined using SPSS. Pearson correlation analyses were also performed with log ($x + 1$)-transformed percent cover data for organismal groups. For the highest Pearson correlations, linear regression was performed using Excel (Microsoft Corporation) and confirmed using SPSS. Nonparametric Spearman's (ρ) correlations were also performed and are presented for comparison in Tables S10, S11, S13, and S14.

Nonparametric, multivariate analyses using PRIMER-e v. 7 (Quest Research Limited) were performed to compare macroalgal and overall species assemblages across sample sites with specific statistical methodology following

recommendations of Clarke et al. (2014). Because percent cover varied by several orders of magnitude across samples, these data were square-root-transformed to down-weight the influence of the most abundant species. Presence-absence of fleshy (i.e., not encrusting) macroalgal species across sites based on diver collections were also compared. Differences among sites were analyzed using PERMANOVA with site as a fixed factor and transects being a random factor nested within site, based on Bray-Curtis similarity matrices. For the fleshy macroalgal dataset, a dummy variable of 0.1 was added to avoid undefined resemblances at site K where no fleshy macroalgae occurred. To visually compare similarity among sites in both percent cover and presence-absence datasets, non-metric multidimensional scaling (nMDS) ordination plots were created based on the resemblance matrix. The nMDS ordinations of fleshy macroalgal assemblages alone included 0.05 metric proportions to fix collapses as recommended by Clarke et al. (2014). Statistical differences among sites were determined using CLUSTER analysis with similarity profile (SIMPROF) tests ($\alpha = 0.05$). To compare similarity among individual transects within and across sites, CLUSTER analysis and SIMPROF tests were performed. To determine which taxa made the greatest contribution to some of the observed patterns, we used species contributions to sample (dis)similarities (SIMPER) tests.

2.6. Hindcasting and forecasting macroalgal cover from sea ice records and predictions

Historical summer Sea Ice Index data for sliding 5-year intervals from 1979 to 2019 were used for hindcasting macroalgal percent covers at each site. The linear regression equation with transects averaged at each site (see Results) was used. The differences between the 2019 macroalgal cover at each site and the regression line were calculated and used to adjust the hindcasted predictions to maintain the same relative difference to the regression line as observed in 2019. Similarly, forecasts of future macroalgal covers at sea ice cover levels that were 15%, 30%, and 50% lower than current levels were calculated using the summer Sea Ice Index regression with untransformed macroalgal cover, the National Ice Center data regression with log-transformed macroalgal cover (see Results), and the annual AMSR2 NASA Team 2 regression with untransformed macroalgal cover (see Results). Because the maximum overall site macroalgal percent cover data in 2019 did not exceed 80% (see Results), this value was used as an upper limit of possible future macroalgal cover levels.

3. Results

3.1. Macroalgal distribution and cover

A total of 36 species of fleshy macroalgae were identified, with 35 of them from the by-hand collections (Table 1). The additional species was *Ascoseira mirabilis* for which one individual was identified with confidence in a video recording from site B. Although *Lambia antarctica*, the only subtidal green alga present in the survey, was not present in the diver collections at sites C, G, or H, a few

Table 1. Species list of macroalgae from by-hand collections

Species	Sites														Total Sites
	A	B	C	D	E	F	G	H	I	J	K	L	M	N	
Total Species:	23	26	17	20	16	20	22	14	7	18	0	4	4	2	
Phaeophyceae															
<i>Desmarestia menziesii</i>	+	+	+	+	+	+	+	+	+	+	-	+	+	+	13
<i>Himantothallus grandifolius</i>	+	+	+	+	+	+	-	+	+	+	-	-	-	-	9
<i>Desmarestia antarctica</i>	+	+	+	+	-	+	-	-	-	+	-	-	-	-	6
<i>Cystosphaera jacquinotii</i>	+	+	+	+	-	-	-	-	-	-	-	-	-	-	4
<i>Desmarestia anceps</i>	+	+	-	-	-	-	+	-	-	-	-	-	-	-	3
<i>Adenocystis utricularis</i>	-	-	-	-	-	+	-	-	-	-	-	-	+	-	2
<i>Ascoseira mirabilis</i>	-	(+) ^a	-	-	-	-	-	-	-	-	-	-	-	-	1
<i>Microzonia australe</i> ^b	-	+	-	-	-	-	-	-	-	-	-	-	-	-	1
Rhodophyceae															
<i>Iridaea cordata</i> ^b	+	+	+	+	+	+	+	+	+	+	-	-	+	-	11
<i>Callophyllis atrosanguinea</i>	-	+	-	+	-	+	+	+	+	+	-	+	+	-	9
<i>Myriogramme mangini</i>	+	+	+	+	+	+	+	+	-	+	-	-	-	-	9
<i>Pantoneura plocamioides</i>	+	+	+	+	+	+	+	+	-	+	-	-	-	-	9
<i>Picconiella plumosa</i>	+	+	+	+	+	+	+	+	-	+	-	-	-	-	9
<i>Plocamium</i> sp. ^b	+	+	+	+	+	+	+	+	-	+	-	-	-	-	9
<i>Georgiella confluens</i>	+	+	+	+	-	+	+	+	-	+	-	-	-	-	8
<i>Myriogramme smithii</i>	+	+	+	+	+	+	+	-	-	+	-	-	-	-	8
<i>Sarcopeltis antarctica</i> ^b	+	+	+	+	+	+	+	-	-	+	-	-	-	-	8
<i>Trematocarpus antarcticus</i>	+	+	+	+	-	+	+	+	+	-	-	-	-	-	8
<i>Hymenocladopsis</i> sp. or spp. ^b	-	+	-	+	+	-	+	+	-	+	-	+	-	-	7
<i>Paraglossum salicifolium</i> ^b	+	+	-	+	-	+	+	+	-	+	-	-	-	-	7
<i>Palmaria decipiens</i>	+	-	+	+	+	-	-	-	+	+	-	-	-	-	6
<i>Curdiea racovitzae</i>	+	+	+	+	+	-	-	-	-	-	-	-	-	-	5
<i>Gymnogongrus antarcticus</i>	+	+	+	-	-	-	+	-	-	-	-	-	-	-	4
<i>Phycodrys austrogeorgica</i>	-	+	-	-	+	+	+	-	-	-	-	-	-	-	4
<i>Porphyra plocamiestris</i>	-	-	-	+	-	+	+	-	-	+	-	-	-	-	4
Undescribed Kallymeniaceae sp. ^b	+	-	-	-	+	-	+	+	-	-	-	-	-	-	4
<i>Austropugetia crassa</i>	+	+	-	-	-	+	-	-	-	-	-	-	-	-	3
<i>Gymnogongrus turquetii</i>	-	-	-	-	+	-	+	-	-	+	-	-	-	-	3
<i>Phyllophora antarctica</i>	-	-	-	-	+	-	-	-	-	-	-	+	-	+	3
<i>Meridionella antarctica</i> ^b	+	+	-	-	-	-	-	-	-	-	-	-	-	-	2
<i>Leniea lubrica</i> ^b	-	-	-	-	-	-	+	-	+	-	-	-	-	-	2
<i>Pachymenia orbicularis</i> ^b	-	+	-	-	-	+	-	-	-	-	-	-	-	-	2
<i>Ballia callitricha</i>	+	-	-	-	-	-	-	-	-	-	-	-	-	-	1
<i>Delisea pulchra</i> ^b	-	-	-	-	-	+	-	-	-	-	-	-	-	-	1
<i>Paraglossum amsler</i> ^b	-	-	-	-	-	-	-	-	-	+	-	-	-	-	1
unidentifiable red blade(s)	+	+	-	+	-	-	+	-	-	-	-	-	-	-	4
Ulvophyceae															
<i>Lambia antarctica</i>	+	+	(+)	-	-	+	(+)	(+)	-	+	-	-	-	-	7

^a(+) indicates that the observation is from the video recordings, not by-hand collection.

^bSee Appendix S2 for notes on macroalgal nomenclature.

individuals of it were identified with confidence in videos at these sites. The most widespread species was *Desmarestia menziesii*, which was collected at all sites except for site K, at which no fleshy macroalgae were observed. *Iridaea cordata* was collected from 11 of the 14 sites, and 12 additional species were collected at eight or more of the 14 sites (Table 1).

Composition of fleshy macroalgal cover differed across sites (PERMANOVA, pseudo- $F_{13,25} = 8.646$, $p(\text{perm}) = 0.001$). A CLUSTER analysis of Bray-Curtis similarities based on the presence of species at each site from diver collections with SIMPROF test revealed three groups of sites that were apparent in an nMDS plot of the similarities (Figure 3a). Sites A through H and J, which contained between 14 and 26 species (Table 1) with an average similarity of 70.4% in SIMPER analysis, clustered tightly together in a single SIMPROF group, while sites I, L, M, and N, which contained two to seven species (Table 1) and an average similarity of 43.9%, formed another significant but less tight cluster (Figure 3a). These two SIMPROF groups had an average dissimilarity of 76.4% in a SIMPER analysis. Site K separated with 100% dissimilarity to the other two groups as it contained no fleshy macroalgae. The same overall pattern and SIMPROF groupings were also observed when the percent cover data from

video analyses for fleshy macroalgae alone were analyzed in the same manner (Figure 3b), although the average dissimilarity in SIMPER analysis was greater with 87.2% and the two groups had slightly lower average similarities of 52.4% and 37.4%, respectively. In addition, the species responsible for the dissimilarities were somewhat different between the two datasets. In the diver-collected presence-absence data, 17 species were cumulatively responsible for over 70% of the dissimilarity with none individually responsible for more than 5.65% (Table S3). In contrast, in the SIMPER analysis of video-based percent cover data, *Himantothallus grandifolius* and *Plocamium* sp. accounted for over 34% of the dissimilarity with only five additional species cumulatively responsible for over 70% of the dissimilarity (Table S4). CLUSTER analysis with SIMPROF test of fleshy macroalgal cover in individual transects revealed that transects within each site usually, but not always, clustered closest together (Figure 4a). When transects from a site did not cluster together, they were still with transects from sites that were in the same SIMPROF group for sites overall (Figure 3). An exception was the transects at site K, which had no fleshy macroalgae and which grouped with transects from site N also with no or almost no fleshy macroalgae.

Fleshy macroalgal cover ranged from 0% to approximately 80% across sites and transects (Figure 5; Table S5). These differences across sites were statistically significant ($F_{13,25} = 37.672$, $p < 0.001$), although in post hoc analyses no site was significantly different from all others (Figure 5). Brown macroalgae tended to be relatively more abundant in transects with higher overall cover except at sites C, D, and H (Figure 5). Although seven sites had the green macroalga *Lambia antarctica* present, it was present at >0.5% cover overall only in the three transects at site B (Figure 5). At most sites, the depth distribution of the algae was similar for both the horizontal transect components (Figure 6) and vertical transect intervals (Figure S2). The only site where significant differences among depths were observed in the horizontal components was site B, where the 30 m and 35 m transects had lower cover than the 10 m and 15 m transects (Figure 6). However, sites G, J, and L had nearly significant differences among depths ($0.05 < p < 0.09$; Figure 6).

Crustose coralline red algae (otherwise unidentified but likely several different species) were observed in video transects at all sites, and non-calcified crustose red macroalgae (*Hildenbrandia* sp. and, possibly, *Gania mollis*) were observed at all sites except for site K (Figure 7). As noted previously, percent cover of encrusting red algae was only calculated using random points that did not have larger, non-encrusting organisms present and that were on hard substrate. Their combined cover in individual transects ranged from <20% to >95% across sites (Figure 7), and the overall site means ranged from approximately 25% to 90% (Table S6). Although there were significant differences in total encrusting red algal cover across sites ($F_{13,25} = 7.828$, $p < 0.001$), there were no clear spatial patterns in these significant differences across the sites (Figure 7).

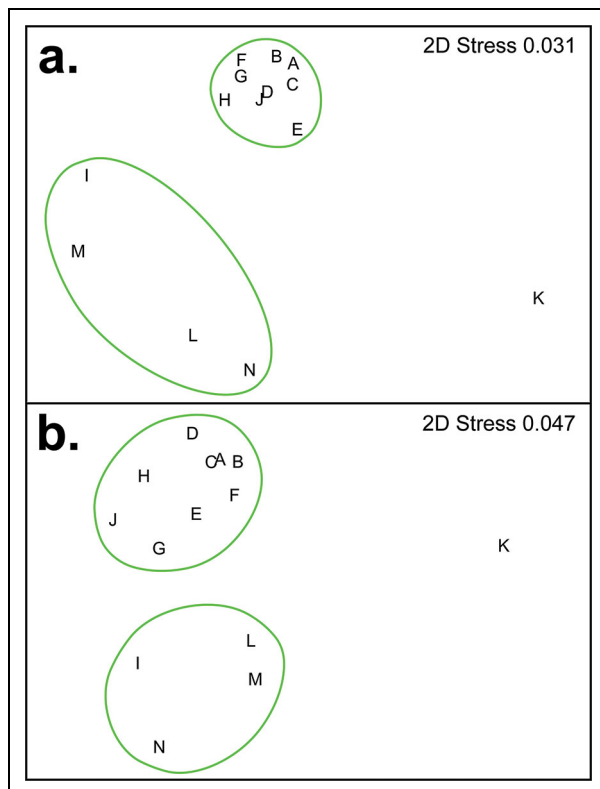


Figure 3. Non-metric multidimensional scaling plots of macroalgal community similarity. These plots are based on: (a) macroalgal presence-absence from diver collections; and (b) macroalgal percent cover from video analyses. Letters indicate study sites (Figure 1; Table S1); green lines separate statistically different site groupings by SIMPROF tests ($p \leq 0.05$).

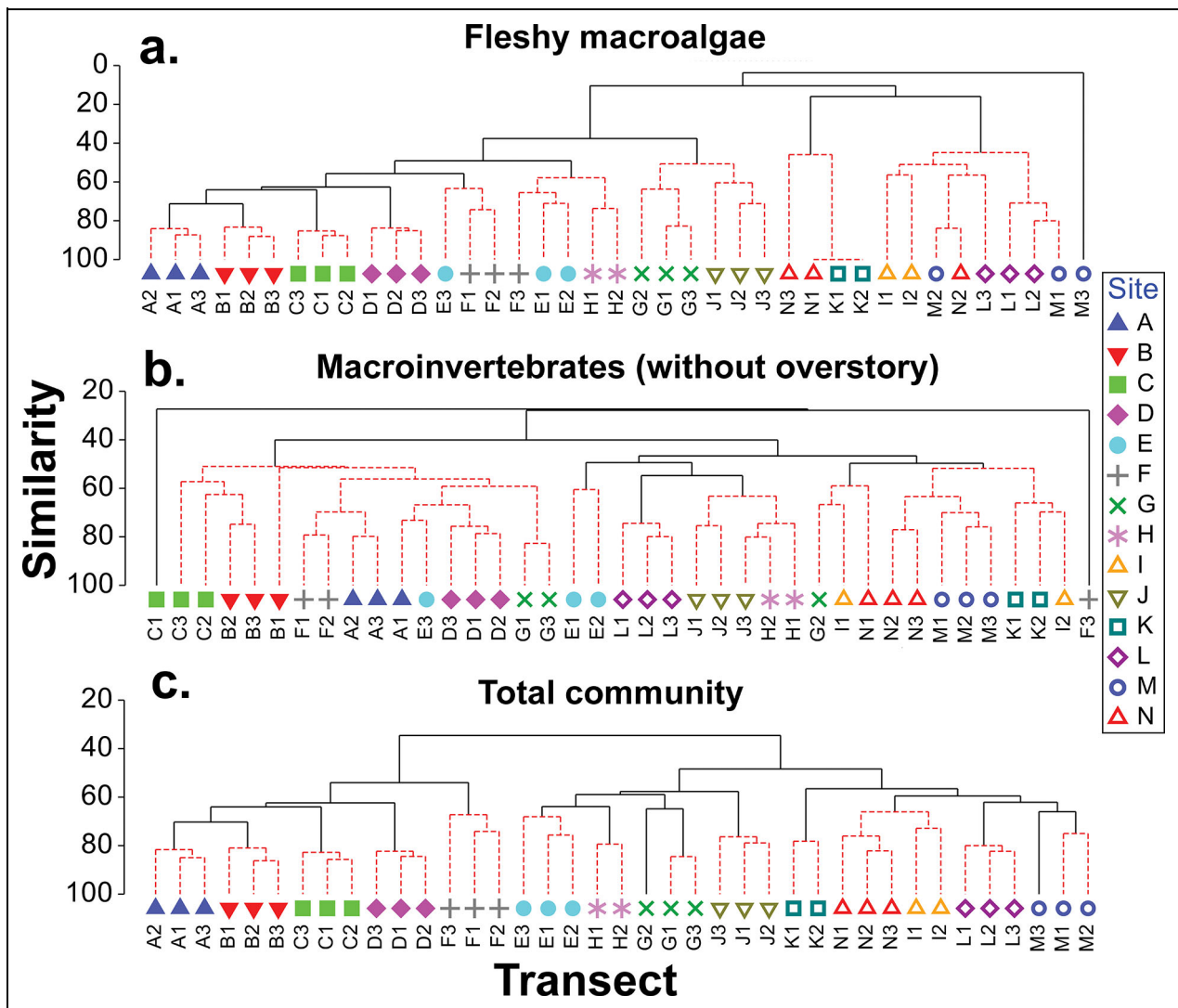


Figure 4. CLUSTER analyses with SIMPROF tests by individual transect. (a) Fleshy macroalgae only; (b) macroinvertebrates without overstory brown macroalgae; and (c) total community. Red dotted lines indicate clusters that are not significantly different ($p > 0.05$).

3.2. Macroinvertebrate distribution and cover

A total of 19 discrete species of macroinvertebrates, plus two species pairs that each could only be assigned to genus, could be confidently identified in the video recordings (Tables 2 and S2). Ten additional taxa (Table 2) were counted, but individuals within them could not be confidently identified to species in the videos. The sea star *Odontaster validus* and limpet *Nacella concinna* were present at all sites (Table 2). Sponges were also present at all sites, but the only individual species that could be consistently identified with confidence in the videos was *Dendrilla antarctica* at five of the sites (Table 2). Table 2 also includes records of 17 invertebrate taxa that were collected at a site by divers for food web analyses (to be published separately) but were not identified under a random dot in the video analysis of that site. These taxa were specifically targeted in the general collections, and some such as *Margarella antarctica*, which was included as “other molluscs” in Table 2, were mesoinvertebrates too small to be readily identified in the videos. Holothuroids

and polychaetes were also taxa that were primarily associated with cracks in the rocks and/or with macroalgal holdfasts and would not have been easily visible in the videos. They were primarily recovered with airlift sampling.

As noted previously, calculations of macroinvertebrate percent cover excluded points with overstory algae. There was a significant difference in macroinvertebrate composition among sites (PERMANOVA, pseudo- $F_{13,25} = 6.322$, $p(\text{perm}) = 0.001$). A CLUSTER analysis of Bray-Curtis similarities of the percent cover of invertebrate species at each site with SIMPROF test revealed two groups of sites that were apparent in an nMDS plot of the similarities (Figure 8). Sites C and F, which were two of the three sites with the fewest macroinvertebrate species in video analyses (Table 2), clustered separately from the rest with average similarity of 49.8% in SIMPER analysis. The remaining sites had an average similarity of 52.9%, and the two groups had an average dissimilarity of 59.9%. The species contributing the most to both within-group similarities

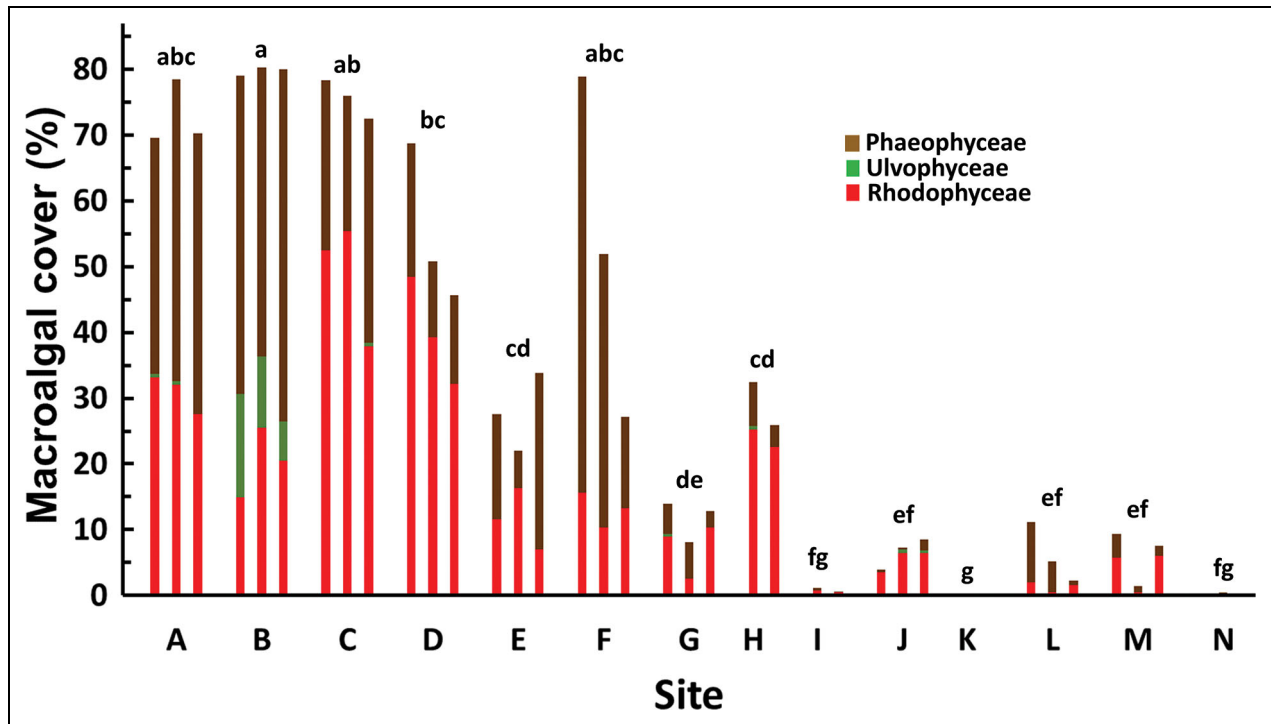


Figure 5. Percent cover of fleshy macroalgae for individual transects at each site. Overall differences across sites were detected in a General Linear Models test (see text), with post hoc analysis results indicated by lower case letters above depth clusters. Sites with the same letter are not significantly different ($p > 0.05$).

and between-group dissimilarities are presented in Table S6. CLUSTER analysis with SIMPROF test of macroinvertebrate cover in individual transects revealed that transects within each site only clustered closest together at sites D, E, L, and M but usually clustered within the same SIMPROF group, with the exceptions being sites C, F, G, I, and N (Figure 4b). Although sites C and F were in a separate SIMPROF group from all other sites overall (Figure 8), in each case two of the three individual transects were in the same SIMPROF group with all three individual transects from sites A, B, and D and one or two transects from sites E and G (Figure 4b).

Macroinvertebrate cover (from parts of imagery without overstory) differed significantly ($H_{13} = 27.104$, $p = 0.012$) across sites (Figure 9). Overall mean cover varied widely across sites from $1.2\% \pm 0.3\%$ (mean \pm S.E., $n = 3$) at site C to $24.2\% \pm 0.9\%$ ($n = 3$) at site L (Table S5). Nonparametric, pairwise comparisons of sites with three transects revealed significant differences (though not with type I error correction), but although the higher percent covers tended to be to the south, no clear trends in overall percent covers were apparent (Figure 9). The most common overall invertebrate groups were sponges, echinoderms, mollusks, ascidians, and bryozoans (Figure 9). The percent cover of all groups differed significantly among sites (echinoderms $H_{13} = 30.813$, $p = 0.004$; mollusks $H_{13} = 31.714$, $p = 0.003$; ascidians $H_{13} = 25.859$, $p = 0.018$; bryozoans $H_{13} = 24.141$, $p = 0.030$) with only the cover of sponges transformable to meet parametric statistical assumptions ($F_{13,25} = 2.337$, $p = 0.033$). In post hoc comparisons of percent covers of individual invertebrate groups, although significant differences were found

among sites (although not with type I error correction for the pairwise, nonparametric comparisons), there were few clear patterns other than those mirroring the overall covers at each site (Figure 9; Table S7). The exception was a pattern of higher cover of echinoderms at the more southerly sites (Table S7). Examination of the raw data revealed that much of this pattern was because of the regular sea urchin *Sterechinus neumayeri*, which had no or little cover in the northern sites but contributed a quarter to nearly half of the total invertebrate cover at sites K through N (Figure S3).

At most sites, there were no significant differences in invertebrate cover among depths in the horizontal transect components (Figure 10) or vertical transect intervals (Figure S4), although there were often trends for higher cover at deeper depths. This trend was significant for both horizontal components and vertical intervals at site L (Figure 10; Figure S4), with the same weaker but significant pattern in the horizontal components at site D (Figure 10). There were also significant differences across depths in the vertical intervals at site A, but the only two depths intervals that differed in post hoc comparisons were 16–19 m being higher than 21–24 m (Figure S4).

3.3. Bare space distribution

All sites were dominated by hard substrate, most commonly bedrock. In the video analyses, as noted previously, space unoccupied by organisms was scored either as unambiguous bare rock or as rock that appeared to have overlying sediment. However, because determining whether or not sediment was present was often very difficult at the 4K resolution of the video images, the

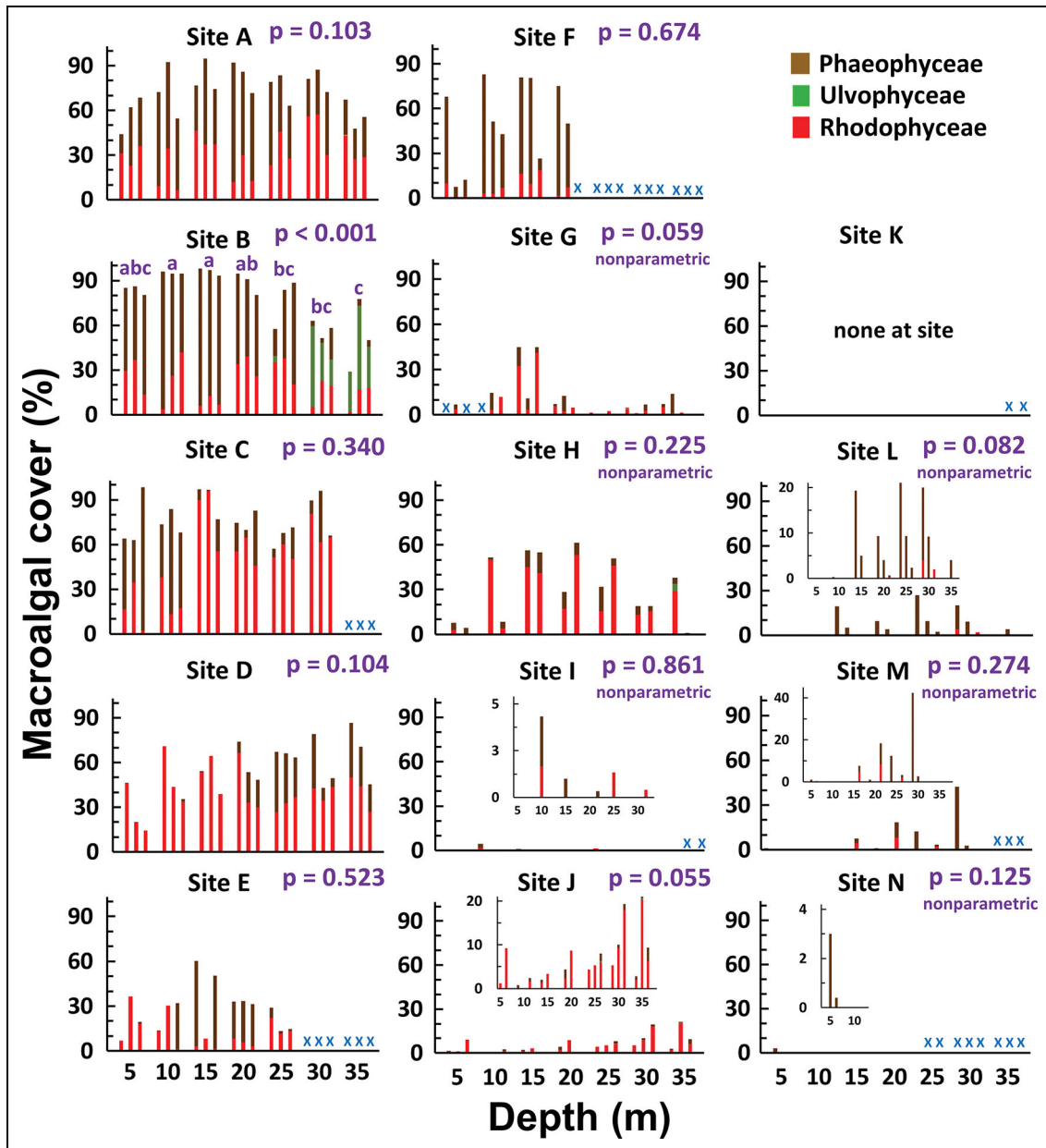


Figure 6. Fleshy macroalgal percent cover in horizontal transect components for individual transects at each site. Blue x letters indicate depths not sampled or data missing (see Methods section). For sites with low overall cover, insets are included with smaller cover scales. Significance levels (p) indicate the results of General Linear Model (parametric) or Kruskal-Wallis (nonparametric) tests. The test statistics by site were: A, $F_{6,14} = 2.221$; B, $F_{6,14} = 11.558$; C, $F_{5,12} = 1.264$; D, $F_{6,14} = 2.206$; E, $F_{4,10} = 0.885$; F, $F_{3,7} = 0.882$; G, $H_6 = 11.698$; H, $H_6 = 8.189$; I, $H_5 = 1.913$; J, $F_{6,14} = 2.768$; L, $H_6 = 11.209$; M, $H_5 = 6.347$; N, $H_4 = 7.222$. Where significant differences were detected, post hoc analysis results are indicated by lower case letters above depth clusters (site B). Depths with the same letter are not significantly different ($p > 0.05$).

distinction between bare rock and rock with sediment should be viewed with caution. Combined bare space differed significantly among sites ($F_{13,25} = 9.562$, $p < 0.001$). Although sites with more bare space tended to be more common to the south, overall there was no clear pattern to bare space across sites (Table S5; Figure S5). There was significant variation among sites in the ratio of unambiguous bare rock to rock apparently with sediment ($H_{13} = 29.121$, $p = 0.006$). Nonparametric, pairwise comparisons of sites with three transects revealed that site G had a significantly lower ratio than all other sites (though not with

type I error correction), but there was no overall pattern with latitude across the remaining sites (Figure S5).

3.4. Overall community distribution

The overall community including macroalgae and invertebrates differed significantly among sites (PERMANOVA, pseudo- $F_{13,25} = 14.332$, $p(\text{perm}) = 0.001$). A CLUSTER analysis of the total community (fleshy macroalgae, encrusting red macroalgae, and macroinvertebrates; original data with all analysis points for each) with SIMPROF test revealed three groups of sites that were apparent on

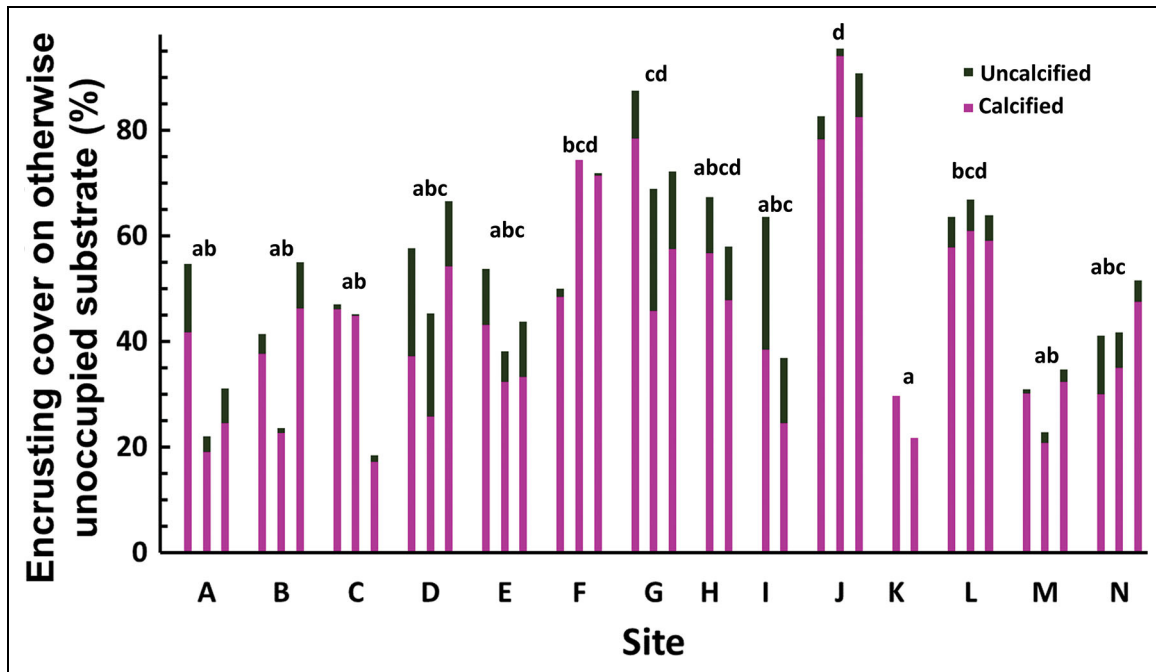


Figure 7. Percent cover of encrusting red macroalgae. Data from hard substrate without overlying organisms by transect at each site. Overall differences across sites were detected in a General Linear Models test (see text), with post hoc analysis results indicated by lower case letters above depth clusters. Sites with the same letter are not significantly different ($p > 0.05$).

an nMDS plot of the similarities (**Figure 11**). Sites A, B, C, D and F clustered together with 64.1% average similarity in SIMPER analysis; sites E, G, H, and J clustered together with 65.1% average similarity; and sites I, K, L, and M clustered together with 61.5% average similarity. The average dissimilarity between the ABCDF group and IKLM group was 73.4%. The EGHJ group had average dissimilarities of 49.6% with both of the other groups. Taxa primarily responsible for the similarities and dissimilarities are listed in Table S8. When the analysis was repeated without including points with the overstory brown macroalgae (but including red and smaller brown macroalgae), site F grouped with the EGHJ group instead of sites A through D (Figure S6). CLUSTER analysis with SIMPROF test of total community cover in individual transects revealed that transects at all sites clustered together (**Figure 4c**). Sites G and M each had one transect that differed significantly from the other two, and all transects at all sites were significantly different from all other sites except for sites I and N, which clustered within the same SIMPROF group (**Figure 4c**). When the analysis was repeated without points with the overstory brown macroalgae, transects clustered together in separate SIMPROF groups, except that one transect from site G clustered with the two transects at site I (Figure S7).

3.5. Correlations between organismal cover, species diversity, species richness, and sea ice cover

The eight sea ice cover metrics used for each site, averaged over the period 2014–2019, are listed in Table S9. The rationale for using 5-year averages and relative attributes of the sea ice metrics are discussed in Appendix S3. Fleшы

macroalgal cover was strongly, negatively correlated with all eight sea ice cover metrics (Table S10). Overall, the highest negative correlations were of log ($x + 1$)-transformed fleshy macroalgal cover (range $r = -0.821$ to -0.891), with the strongest correlation to the annual National Ice Center dataset (**Figure 12a**). The ranges of correlations were slightly lower for correlations to the untransformed cover data (range $r = -0.791$ to -0.880). The strongest untransformed correlations ($r = -0.880$) were with the summer SII and annual AMSR2 NASA Team 2 datasets (**Figure 12b** and **c**). For simplicity of comparisons, all figures for correlations of the various biological metrics with sea ice concentration have been plotted against one of these three datasets—whichever had the stronger correlation—even though other sea ice datasets may have had stronger correlations as shown in the supplementary tables. Encrusting red macroalgal percent cover did not correlate significantly with any of the eight sea ice datasets (Table S10; Figure S8a). There were also no significant correlations between macroinvertebrate percent cover and any of the eight sea ice datasets (Table S11; Figure S8b). The highest correlation was between log-transformed macroinvertebrate cover and the annual SII dataset ($r = 0.454$, $p = 0.103$).

Neither encrusting red algal percent cover nor macroinvertebrate cover correlated significantly with fleshy macroalgal cover (Table S12; Figure S9). The correlation between the log of macroinvertebrate cover and untransformed macroalgal cover was close to the level of statistical significance ($r = -0.489$, $p = 0.076$; Table S12).

Shannon diversity of macroinvertebrates (by percent cover without overstory) was significantly, positively

Table 2. Taxa of macroinvertebrates identified in video analysis of the transects

Taxa	Sites														Total Sites
	A	B	C	D	E	F	G	H	I	J	K	L	M	N	
Total Taxa:	11	10	9	13	9	7	14	15	12	13	15	18	13	12	
Porifera															
<i>Dendrilla antarctica</i>	(+) ^a	(+)	(+)	(+)	+	(+)	(+)	+	-	+	-	+	(+)	+	5
Other sponges	+	+	+	+	+	+	+	+	+	+	+	+	+	+	14
Cnidaria															
Hydroid	-	-	-	+	+	-	+	+	+	+	+	+	+	+	10
Alcyonariid	(+)	(+)	-	(+)	-	-	(+)	-	-	(+)	-	(+)	+	+	2
Anemone	+	-	-	+	+	(+)	(+)	(+)	-	-	+	+	+	-	6
Nemertea															
<i>Parborlasia corrugatus</i>	-	-	-	-	-	-	-	+	-	-	-	-	-	+	2
Mollusca															
<i>Adamussium colbecki</i>	-	-	-	-	-	-	-	-	-	-	(+)	-	-	+	1
<i>Austroborlasia kerguelensis</i>	(+)	-	-	(+)	(+)	(+)	+	-	(+)	(+)	-	-	-	-	1
<i>Marseniopsis mollis</i>	-	-	-	-	-	-	-	-	-	+	(+)	(+)	(+)	-	1
<i>Nacella concinna</i>	+	+	+	+	+	+	+	+	+	+	+	+	+	+	14
<i>Tritoniella belli</i>	-	-	-	-	-	-	(+)	-	-	-	-	+	-	-	1
Other mollusks	+	(+)	(+)	+	(+)	+	-	-	(+)	(+)	-	+	+	-	5
Echinodermata															
<i>Acodontaster</i> sp.	-	-	-	-	-	-	+	+	+	-	+	+	-	-	5
<i>Cuenotaster involutus</i>	-	-	-	-	-	-	+	-	+	-	(+)	-	(+)	-	2
<i>Diplasterias</i> spp.	+	+	+	+	(+)	+	+	+	+	(+)	+	+	(+)	-	10
<i>Granaster nutrix</i>	-	-	-	+	-	-	-	-	-	+	-	-	-	-	2
<i>Labidiaster annulatus</i>	-	+	+	+	-	-	(+)	-	(+)	-	+	(+)	-	-	4
<i>Neosmilaster georgianus</i>	+	+	(+)	+	(+)	(+)	(+)	+	(+)	+	+	-	(+)	-	6
<i>Odontaster meridionalis</i>	-	-	+	-	-	+	-	+	-	-	-	-	-	-	3
<i>Odontaster validus</i>	+	+	+	+	+	+	+	+	+	+	+	+	+	+	14
<i>Perknaster</i> spp.	+	(+)	(+)	+	(+)	(+)	-	-	-	+	(+)	(+)	(+)	-	3
<i>Macroptychaster accrescens</i>	+	-	-	-	-	-	-	-	-	-	-	+	-	-	2
<i>Ophionotus victoriae</i>	-	-	-	-	-	-	+	-	+	-	+	+	+	+	6
<i>Promachocrinus kerguelensis</i>	-	-	-	-	-	-	+	-	+	-	+	+	-	-	4
<i>Sterechinus neumayeri</i>	(+)	+	-	-	(+)	(+)	+	+	+	+	+	+	+	+	9
Holothuroid	(+)	-	-	(+)	-	-	-	-	-	-	-	+	+	(+)	2
Ascidia															
<i>Cnemidocarpa</i> sp.	(+)	+	+	+	+	(+)	(+)	+	+	+	+	+	+	+	11
Other ascidians	+	-	+	-	+	-	+	+	-	+	+	+	+	+	10
Other groups															
Bryozoan	+	+	+	+	+	+	+	+	+	+	+	+	+	-	13
Brachiopods	-	-	-	-	-	-	(+)	+	-	-	-	-	-	-	1
Polychaetes	-	-	(+)	(+)	(+)	(+)	+	(+)	(+)	(+)	(+)	(+)	(+)	(+)	1

^a (+) indicates that these taxa were present in general or airlift collections at the site, even though not identifiable under a random point in the video analyses. The sums for Total Taxa and Total Sites are based only on video analysis.

correlated with seven of the eight sea ice cover metrics and nearly so ($p = 0.053$) in the other (Figure 13a; Table S13). Species richness of macroinvertebrates was not significantly correlated with any sea ice metric (Figure 13b; Table S13). Shannon diversity of the overall community (by percent cover) was significantly, negatively correlated with all eight sea ice cover metrics (Figure 13c; Table S13). Species richness of the overall community was also significantly, negatively correlated with all eight sea ice metrics (Figure 13d; Table S13). Shannon diversity of macroinvertebrates was significantly, negatively correlated to both untransformed and $\log(x + 1)$ -transformed fleshy macroalgal cover (Table 3; Figure 14a). Macroinvertebrate species richness was significantly, negatively

correlated with untransformed fleshy macroalgal cover (Table 3; Figure 14b) but not significantly correlated in a test with log-transformed fleshy macroalgal cover data (Table 3). Overall community Shannon diversity correlated positively with fleshy macroalgal cover for both untransformed and log-transformed data (Table 3; Figure 14c). Overall community species richness was significantly, positively correlated with the log of macroalgal cover (Table 3; Figure 14d) but did not meet the level of significance in a test with untransformed macroalgal cover ($p = 0.073$; Table 3).

3.6. Extrapolations to historic sea ice data and to future sea ice predictions

The portion of the Sea Ice Index dataset used in this analysis began in January 1979, decades before either the National Ice Center or AMSR2 datasets. The mean summer sea ice concentration has fluctuated markedly since then at all study sites (Figure S10). Sliding 5-year means at each site reveal that 2019 and the three preceding years had mean annual sea ice concentration 5-year ice histories slightly higher than or in some cases, similar to, much of the satellite record (Figure S11). However, at all sites there were two very low ice cover 5-year periods, ending in 1993 and 2011 (Figure S11). At all sites, the highest sliding 5-year mean ice concentration was the earliest one in the record, ending in 1984, and at most sites the subsequent 1 or 2 years were also higher than any other in the satellite record. Extrapolating from the 2014 to 2019 summer SII linear regression with fleshy macroalgal cover in 2019 (Figure 12b) indicated that macroalgal cover at all sites could have been fluctuating substantially over the past 40 years (Figure 15). At the seven highest sea ice cover sites, the simple calculations would predict an

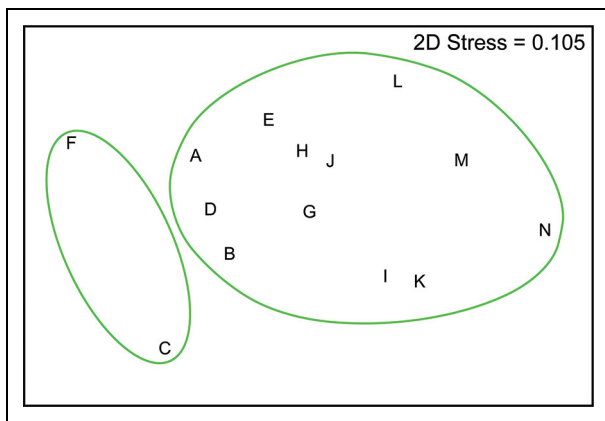


Figure 8. Non-metric multidimensional scaling plot of similarities by site for macroinvertebrates (without overstory). Green lines separate statistically different site groupings by SIMPROF tests ($p \leq 0.05$).

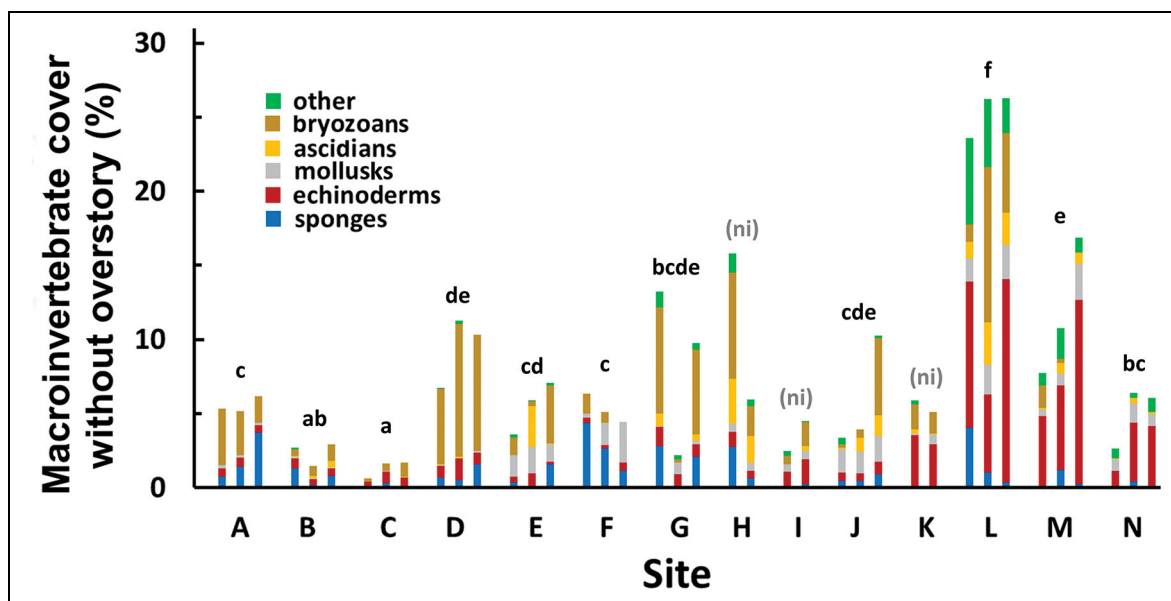


Figure 9. Percent cover of macroinvertebrates by major taxonomic group by transect at each site. Data are only from areas without overstory. Overall differences across sites were detected in a Kruskal-Wallis test (see text), with post hoc analysis results indicated by lower case letters above depth clusters. Sites with the same letter are not significantly different ($p > 0.05$). Some sites (H, I, K) were not included (ni) in the post hoc analyses because they had fewer than three transects.

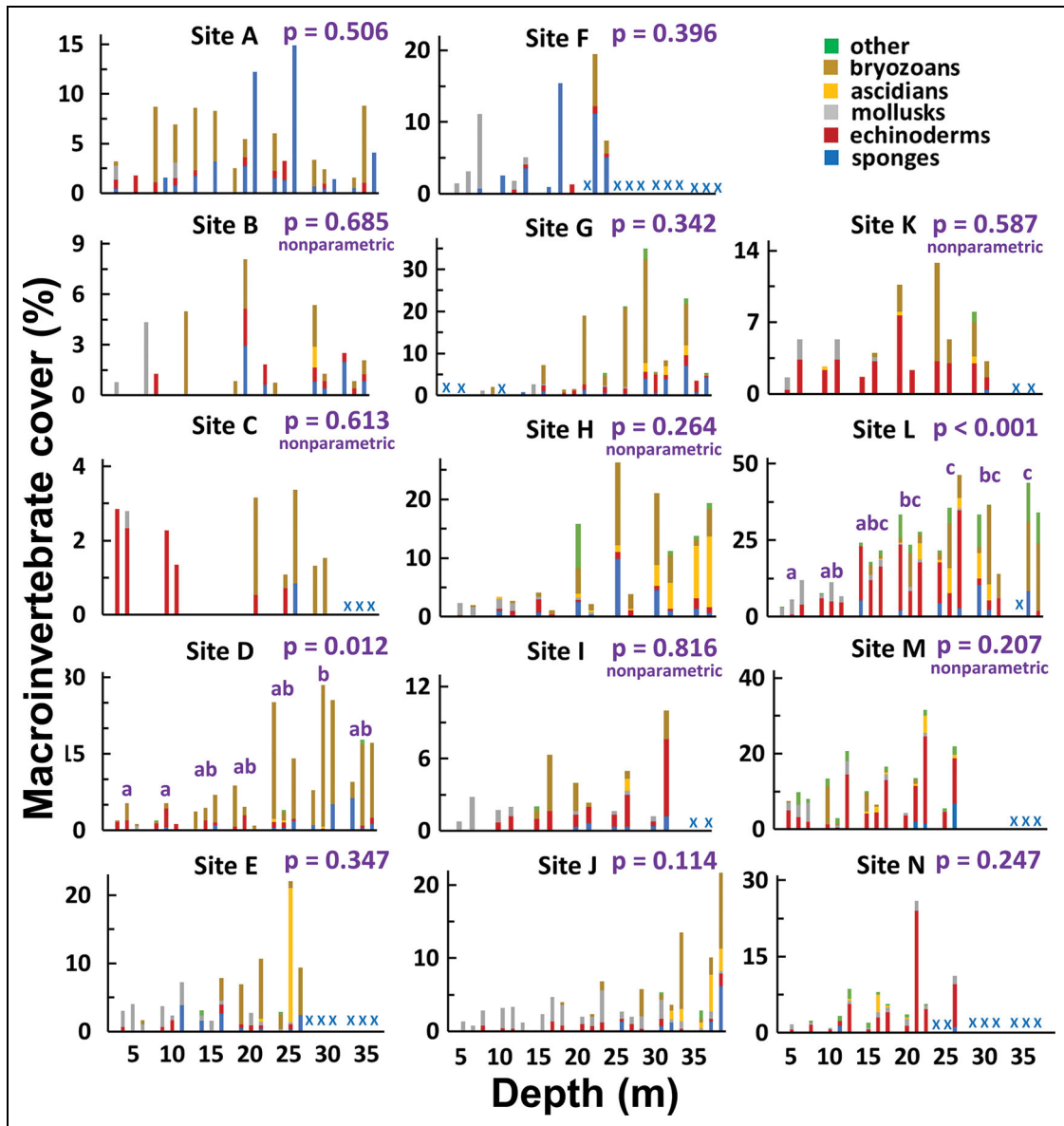


Figure 10. Macroinvertebrate percent cover in horizontal transect components for individual transects at each site. Data are only from areas without overstory. Blue x letters indicate depths not sampled or data missing (see Methods section). Note the different vertical scales in the individual plots. Significance levels (p) indicate the results of General Linear Model (parametric) or Kruskal-Wallis (nonparametric) tests. The test statistics by site were: A, $F_{6,14} = 0.925$; B, $H_6 = 3.938$; C, $H_5 = 3.771$; D, $F_{6,14} = 4.214$; E, $F_{4,10} = 1.261$; F, $F_{3,7} = 1.142$; G, $F_{6,11} = 1.278$; H, $H_6 = 7.657$; I, $H_5 = 2.231$; J, $F_{6,14} = 2.129$; K, $H_5 = 3.745$; L, $F_{6,13} = 8.264$; M, $H_5 = 7.195$; N, $F_{4,8} = 1.676$. Where significant differences were detected, post hoc analysis results are indicated by lower case letters above depth clusters. Depths with the same letter are not significantly different ($p > 0.05$).

absence of macroalgae in 1984 (negative predicted cover), with brief earlier periods of no cover for the two sites, K and N, with the lowest macroalgal cover in 2019 (Figure 15). The highest fleshy macroalgal cover observed in 2019—and, therefore, used in the regression analysis—was approximately 80%, so that projections above that level (purple dashed line on Figure 15) should be viewed with caution. We have also displayed the data as percent changes from 2019 cover levels but included only sites A through H and J, which in 2019 were not significantly different in terms of their macroalgal community composition (Figure 3). Based on this extrapolation, there would

have been relatively little change at the lowest ice cover/highest macroalgal cover sites (A through D) compared to the 2019 cover over the period of the SII record, with greater fluctuations at sites E, F, and H (Figure S12). However, the extrapolations predict possible 4-fold to 8-fold fluctuations at sites G and J (Figure S12), which had the lowest 2019 fleshy macroalgal cover (Figure 5) in this group of sites with similar communities.

Extrapolations of macroalgal cover under future sea ice conditions with 15%, 30%, and 50% lower ice cover than present (Table 4) were performed with the three best overall macroalgal to sea ice cover correlations (Figure 12;

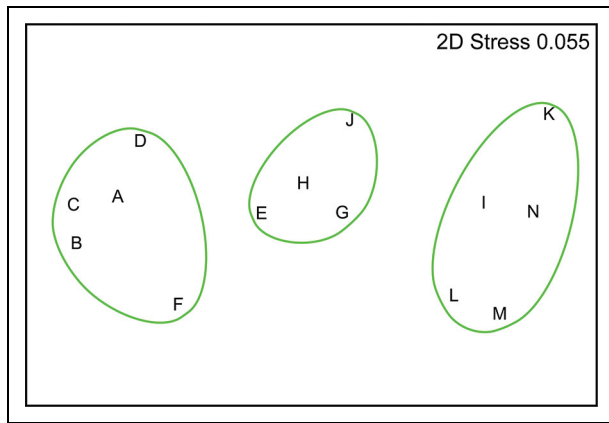


Figure 11. Non-metric multidimensional scaling plot of similarities by site for the overall community by percent cover. Green lines separate statistically different site groupings by SIMPROF tests ($p \leq 0.05$).

Table S9). These correlations were also the best for sea ice concentrations derived from the three underlying raw datasets (National Ice Center, Sea Ice Index, and Advanced Microwave Scanning Radiometer 2; Table S9). The projections using the Sea Ice Index and AMSR2 NASA Team 2 regression equations were similar, with dramatic increases in macroalgal cover predicted at sites with lower 2019 macroalgal cover levels but smaller increases predicted for sites with the highest 2019 cover levels (Table 4). The National Ice Center regression projections, which were based on the log of 2019 macroalgal cover, were higher, often substantially higher, than the other two projections for all but the lower ice cover sites for 15% and some 30% reduced future ice levels and at all but the two lowest 2019 cover sites (K, N) at a 50% reduced ice level.

4. Discussion

4.1. Patterns across study sites

A somewhat unexpected outcome of our nonparametric, multivariate analyses of Bray-Curtis similarities was the clustering of macroalgal assemblages across the northern half of the study area for all but the site with the highest sea ice concentrations (site I). Furthermore, this pattern was evident using either macroalgal species presence-absence data from by-hand collections or macroalgal percent cover by species data from video analyses. By other metrics such as species richness and sea ice cover, the sites varied greatly. However, all of these northern sites contained the two most widespread macroalgal species, the overstory brown alga *Desmarestia menziesii* and shallow-water red alga *Iridaea cordata*. Most or all of these sites also contained *Himantothallus grandifolius*, the next most widespread brown alga, and most of the other more widespread red macroalgae.

As expected, fleshy macroalgal percent cover varied greatly across the study area, with much higher cover in the less ice-covered areas. Amsler et al. (1990, 1995) reported that 85% of the benthos was covered by fleshy macroalgae at five sites near Palmer Station (Figure 1) in proximity to present sites B and C, which was slightly

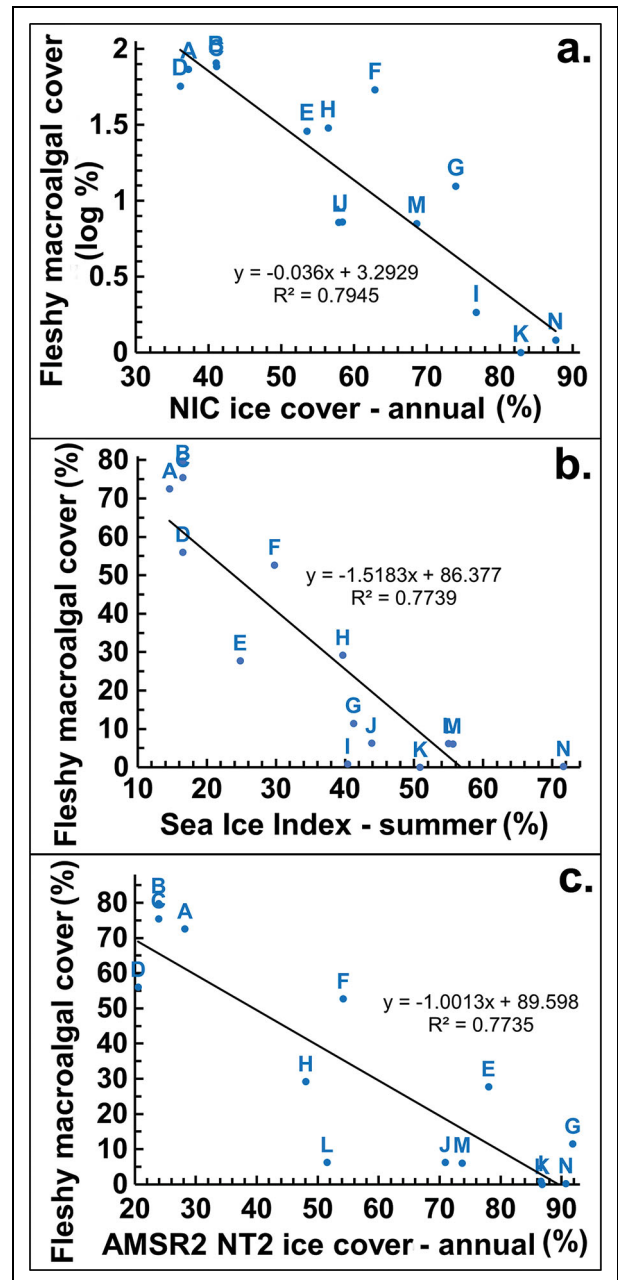


Figure 12. Fleshy macroalgal cover versus three sea ice cover datasets. (a) National Ice Center annual (12-month) ice concentrations; (b) Sea Ice Index summer (October through February) ice concentrations; and (c) AMSR2 NASA Team 2 annual (12-month) sea ice concentrations. Blue points and letters indicate the 14 study sites (Figure 1; Table S1); black lines indicate linear regressions.

higher than observed for overall transects at any of our northern sites. Data from collections in 1989, however, were heavily biased to shallow depths. Two of the 1989 sites were only sampled at depths of 2 m and 5 m, with one additional site each being sampled only to 10 m, 15 m, and 20 m (Amsler et al., 1995). In the present study, site B had percent covers above 80% in this depth range which were significantly higher than deeper depths. The only other report of macroalgal percent cover in our study area

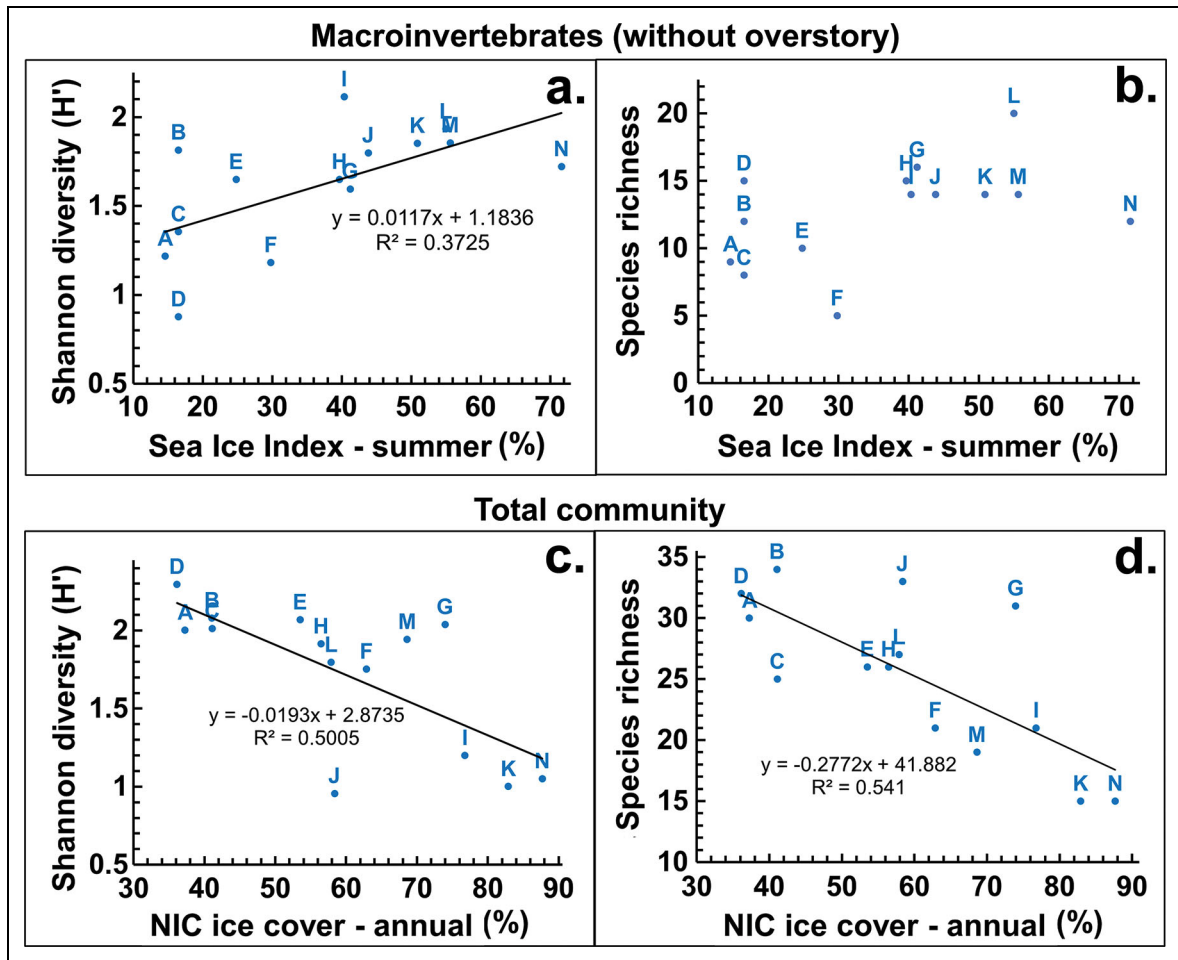


Figure 13. Shannon diversity and species richness for macroinvertebrates and total community versus sea ice concentration datasets. For macroinvertebrates without overstory: (a) Shannon diversity (H') and (b) species richness versus Sea Ice Index summer (October through February) ice concentrations (%); for the total community: (c) Shannon diversity and (d) species richness versus National Ice Center (NIC) annual (12-month) ice concentrations (%). Blue points and letters indicate the 14 study sites (Figure 1; Table S1); black lines indicate linear regressions.

that we are aware of is that of Bowden (2005) who reported on percent cover of benthic flora and fauna at two depths (8 m and 20 m) from three sites near Rothera Station on Adelaide Island (Figure 1). Measures of fleshy macroalgal cover were not presented explicitly but qualitatively reported to be below 2% across sites and depths. Overall macroalgal cover at site L, our site closest to Rothera, was 6.2%. Although the Rothera area and site L are geographically close and similar in sea ice cover, the Rothera sites are in areas that have higher turbidity, at least in January–March (0.104 m^{-1} at site L, 0.130 m^{-1} at Rothera determined as described above), which may account for much of the difference.

Because of the limitations of our video methodology, the absolute levels of encrusting macroalgal cover we have reported should be viewed with caution, and therefore we did not analyze these data further by depth. As described in the methods, any random analysis point with a fleshy macroalga or a macroinvertebrate was excluded from consideration, as was any point that appeared to possibly be on rock covered with sediment, potentially obscuring encrusting organisms below. Nonetheless, we have

reported these data because we believe that the relative levels of encrusting macroalgae across sites should be reasonably comparable even though the sites with lower macroalgal cover had more random points available for these analyses. Also, we have included these data because there are very few reports on encrusting algal cover on the WAP. Amsler et al. (1995) reported crustose algal cover from five sites near Palmer Station with the data collected from photographs of quadrats from which all non-encrusting organisms had been removed. Mean percent cover was 77% with little variation across the 2–20 m depth range sampled. At three sites near Rothera Station, Bowden (2005) reported that encrusting algae were the dominant sessile organisms at 8 m depth, covering 26% of the benthos but decreasing to approximately 11% cover at 20 m, the only other depth sampled. North of our study area on King George Island (62.2°S; Figure 1) we used supplementary data from Valdivia et al. (2014) to calculate that the mean encrusting red algal cover on non-sediment substrates at four sites was approximately 18% at 5–10 m depth and less than 2% at 25–30 m. However, unlike the calculated covers in the present study, these estimates do

Table 3. Parametric Pearson correlations^a of fleshy macroalgal percent cover with both Shannon diversity (H') and species richness (S) for the overall community and for macroinvertebrates alone

Parameter	Statistic	Overall Community		Macroinvertebrates	
		H'	S	H'	S
Fleshy macroalgal cover	r	0.650	0.493	-0.672	-0.584
	p	0.012	0.073	0.009	0.028
Log fleshy macroalgal cover	r	0.812	0.665	-0.680	-0.444
	p	<0.001	0.010	0.008	0.112

^aMain conclusions were based on these correlations, but nonparametric Spearman's correlations are reported for comparison in Table S14.

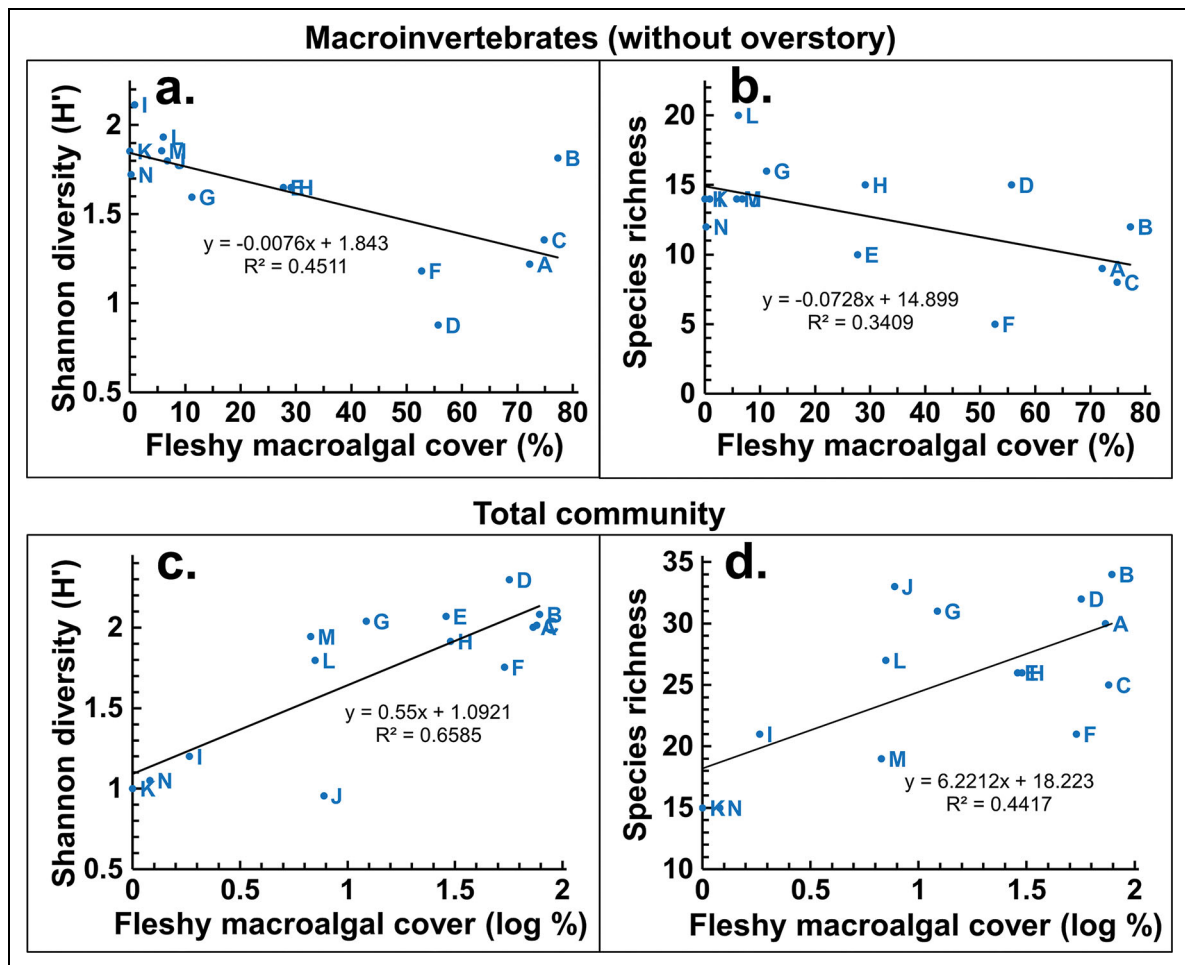


Figure 14. Shannon diversity and species richness for macroinvertebrates and total community versus fleshy macroalgal cover. For macroinvertebrates without overstory: (a) Shannon diversity (H') and (b) species richness versus fleshy macroalgal cover (%); for the total community: (c) Shannon diversity and (d) species richness versus fleshy macroalgal cover (%). Blue points and letters indicate the 14 study sites (Figure 1; Table S1); black lines indicate linear regressions.

not exclude sample points with other organisms. From two other sites on King George Island, Newcombe and Cárdenas (2011) reported that calcified encrusting red algae covered 65%–85% of the rock surface beneath other organisms at 5 m but only 10%–20% at 1 m and 10 m depths. We are not aware of other encrusting macroalgal cover data from the WAP, but a study in East Antarctica (66.2°S, 110.32°E) reported that encrusting coralline

red algae covered 75%–80% of the bottom beneath canopies of *Himantothallus grandifolius* but less than 20% beneath stands of the red alga *Palmaria decipiens* or in areas without overlying macroalgae (Irving et al., 2005). The same study also reported lower photosynthetic rates and bleaching of coralline algae when the *H. grandifolius* canopy was experimentally removed. These findings would suggest that our percent cover data for encrusting

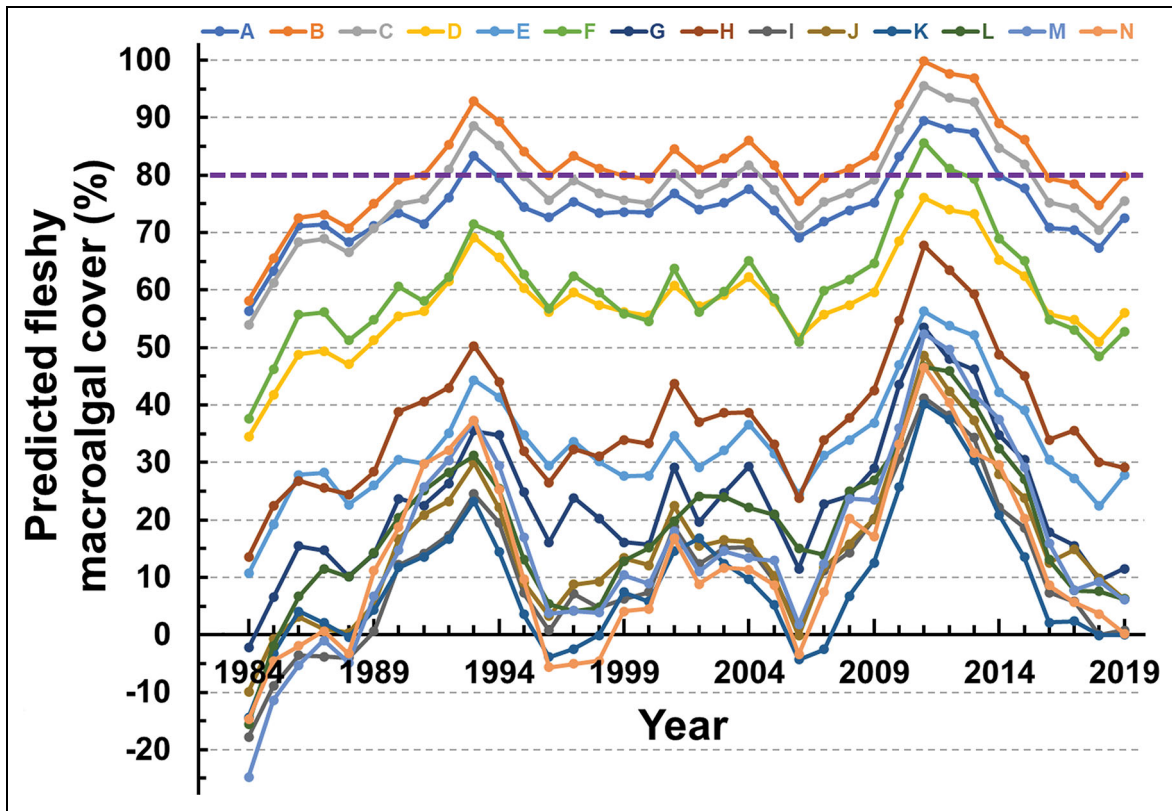


Figure 15. Hindcast projections of past fleshy macroalgal cover from historical summer Sea Ice Index concentrations. Projections are based on past sea ice concentrations (Figures S10 and S11) and the linear regression of 2019 macroalgal cover to the 2015–2019 summer Sea Ice Index dataset. The 2019 data are the actual observed percent covers. Projections for each prior year are based on the mean of the sea ice data from the 5 preceding years. The purple line at 80% cover represents the highest cover observed at transects in 2019, which could be considered the upper limit of confidence for projections.

red algae could be substantial underestimates. However, in the present study we observed no significant correlation between fleshy macroalgal cover and encrusting algal cover, and site J, for example, had nearly 90% cover of encrusting algae even though it had relatively low percent cover of both fleshy macroalgae and macroinvertebrates. The encrusting red algal cover at site J without any correction for overlying organisms or sediment was 67%. Our experience at Palmer Station and also at McMurdo Station (Ross Sea, 77.8°S 164.7°E) is that crustose coralline algae are quite common in areas without overlying organisms.

As described previously, we chose to calculate macroinvertebrate cover without including sample points with overstory brown macroalgae, as that clearly would have underestimated macroinvertebrate cover at sites with high macroalgal cover. Our experience is that some macroinvertebrates along the WAP, particularly echinoderms and mollusks, commonly occur beneath the overstory. However, other macroinvertebrates usually do not occur under overstory macroalgae, which we recognize may have resulted in somewhat artificially high estimates of the cover for them. Our extensive personal observations from the Palmer Station area are that some sponge species, particularly the larger ones, are usually not found with overstory brown macroalgae unless the macroalgal cover is low. However, that is not the case for the most common

sponge by far that we observed in the present study, *Dendrilla antarctica*, which often occurs beneath overstory brown algae (von Salm et al., 2022). Cárdenas et al. (2016) reported that compared to temperate areas, East Antarctica, or the Arctic, canopies of *Desmarestia menziesii*, *D. anceps*, and *Himantothallus grandifolius* on the WAP are characterized by a relatively high sponge species richness between 10 m and 20 m, the only depths sampled. We believe that while some individual taxa may be over-represented via our methodology, the data overall should be representative of the macroinvertebrate assemblages.

Although there were significant differences in macroinvertebrate percent cover among sites, the macroinvertebrate assemblages across the entire study area were determined to be similar based on nonparametric, multivariate analyses of Bray-Curtis similarities. As a whole, sites C and F were separate from the others but when individual transects were compared, two of the three transects at each of these sites clustered with and were not significantly different from many of the transects at other sites. The outliers, transects C1 and F3, had very low similarity with any other transects. Transect C1 had the lowest macroinvertebrate cover of any transect in our study. Transect F3 only covered 5 m to 15 m depth, whereas F1 and F2 continued to 20 m and all other transects in the study continued to 25 m or deeper. Transect F3 had the highest

Table 4. Projections under different climate change sea ice predictions for three different current sea ice versus fleshy macroalgal cover regressions, with a summary of the lowest projection of the three models for each site

Site	2019 cover (%)	Lowest Projection of the Three			Sea Ice Index Summer ^a			National Ice Center Annual ^a			AMSR2 NASA Team 2 Annual ^a		
		15% less	30% less	50% less	15% less	30% less	50% less	15% less	30% less	50% less	15% less	30% less	50% less
A ^b	72.5	76	79	80 ^c	76	79	80*	80*	80*	80*	77	80*	80*
B	79.7	80*	80*	80*	80*	80*	80*	80*	80*	80*	80*	80*	80*
C	75.5	79	80*	80*	79	80*	80*	80*	80*	80*	79	80*	80*
D	56.0	59	62	66	60	64	69	80*	80*	80*	59	62	66
E	27.7	33	39	47	33	39	47	55	80*	80*	39	51	67
F	52.7	60	66	75	59	66	75	80*	80*	80*	61	69	80
G	11.5	21	30	43	21	30	43	30	78	80*	25	39	57
H	29.2	36	44	53	38	47	59	60	80*	80*	36	44	53
I	0.8	4	11	32	10	19	31	4	11	80*	14	27	44
J	6.3	14	26	40	16	26	40	14	30	80*	17	28	42
K	0.0	2	7	30	12	23	39	2	7	30	13	26	43
L	6.2	14	22	32	19	31	48	14	29	78	14	22	32
M	6.1	16	28	43	19	31	48	16	38	80*	17	28	43
N	0.2	3	10	45	17	33	55	3	10	45	14	27	46

^aThe regression for the National Ice Center data was to log-transformed macroalgal cover, while the other two are from regressions of untransformed macroalgal cover.

^bItalics highlight sites A through H and J, which were in the same SIMPROF group of similarities among macroalgal communities across sites (Figure 3). Sites I, L, M, and N were in a second group, and site K, with no fleshy macroalgal cover, differed significantly from all others (Figure 3).

^cProjections of >80% macroalgal cover were adjusted to “80*” because the highest overall transect macroalgal cover in 2019 was slightly less than 80% (Figure 5).

percent cover of mollusks of any transect in our study, comprised exclusively of the limpet *Nacella concinna*, which occurs in highest densities at shallower depths (Brêthes et al., 1994; Barnes and Brockington, 2003; Bowden, 2005). As these two outlier transects drove the statistical difference between sites C and F versus all others, we conclude that the macroinvertebrate assemblages should be considered as quite similar across all sites.

As noted above, the only apparent pattern across study sites in terms of macroinvertebrate cover was the increasing percent cover of echinoderms at more southerly sites (K through N), a pattern driven largely by the regular sea urchin *Sterechinus neumayeri* (Figure S3). White et al. (2012) reported that densities of *S. neumayeri* from five sites near Palmer Station sampled in 1989 ranged from 0 to 8.7 individuals m⁻² (mean of 3.4) but, where present, were almost all small individuals that likely were collected from cracks and between cobble by an airlift sampler. By comparison and consistent with our results, near Rothera Station, Bowden (2005) reported approximately 100 individual *S. neumayeri* m⁻² consistently across depths at three sites. Smale (2008) sampled three depths at each of four Rothera area sites and reported densities of

approximately 40 to 150 individuals m⁻² in all but one of the 12 samples. We are not aware of other reports of *S. neumayeri* densities in our study area, but from Doumer Island, near our site D (Figure 1), Zamorano et al. (1983) reported that this species constituted 12% of the macroinvertebrate biomass between 0 m and 10 m and was also present at 15 m depth. Farther north along the WAP, Arnaud et al. (1986) reported that *S. neumayeri* was relatively common on King George Island (62.2°S) sampled across the broad depth range of 10 m to 600 m. In another part of King George Island, Nonato et al. (2000) reported that densities of *S. neumayeri* ranged from 0 to 10 individuals m⁻² (mean <1) along a transect in sandy sediments from depths of 6 m to 25 m that was sampled over 3 years.

Compared to assemblage similarities for the fleshy macroalgal assemblage alone, comparisons across sites for the overall communities yielded groupings corresponding to sites with high, medium, and low fleshy macroalgae, respectively. This analysis utilized our complete dataset, so for reasons described above could be underrepresenting the macroinvertebrate assemblages at sites with high overstorey macroalgal cover. However, when the analysis was

repeated, excluding data from the overstory brown algae, only site F changed groups (Figure S6).

4.2. Depth-related patterns within study sites

Fleshy macroalgal cover varied little with depth from 5 m to 40 m at our northernmost study sites. At all of the sites throughout the study area where bottom topography allowed divers to reach 40 m depth, we observed fleshy macroalgae continuing to even greater depths. An often-cited study (Gómez et al., 1997) of photosynthetic light requirements of overstory and other fleshy macroalgae at Potter Cove on King George Island indicated that the lower depth limit of fleshy macroalgae should extend deeper than 30 m, yet illustrations of Antarctic macroalgal depth distributions commonly extend only to 30 m (e.g., Gómez and Huovinen, 2020). Early reports of WAP macroalgae from dredged collections as deep as 100 m (e.g., Zieliński, 1990) have usually been assumed to be from drift material dislodged from shallower depths (Wiencke et al., 2014; Robinson et al., 2022). The lower depth distribution of macroalgae reported at Signy Island (60.7°S) was 38 m, the maximum depth observed (Brouwer, 1996b). There are reports from remotely operated vehicle observations of *Himantothallus grandifolius* attached to bedrock at 70 m (Wiencke et al., 2014) and *Palmaria decipiens* attached at 100 m (Robinson et al., 2022). It seems likely that fleshy macroalgae commonly extend much deeper into the WAP benthos than has often been assumed, consistent with the observations in our study. The only sites where we did not find fleshy macroalgae at the greatest depth sampled were the high sea ice sites K, where no fleshy macroalgae occurred, and N, where in video transects we only observed *Desmarestia menziesii* in the 5 m horizontal transect components, although it was also present in by-hand collections at 10 m and 15 m. In addition, *Phyllophora antarctica* was found at site N during general collections in very shallow depths. Similarly, fleshy macroalgae in the Arctic also extend into deeper waters based on remotely operated vehicle and other remote sampling. Krause-Jensen et al. (2019) reported that kelp forests in Greenland extended deeper than 61 m (greatest depth observed) at some offshore sites. Schimani et al. (2022) reported brown macroalgae as deep as 32 m and fleshy red macroalgae as deep as 68 m in Spitsbergen. Myer and Sweetman (2015) reported an abundant but unidentified organism that appeared to be a fleshy macroalga at 166 m in Spitsbergen.

One abiotic variable we could not control that (literally) impacts benthic communities is scouring by icebergs of various sizes which can remove macroalgae and sessile macroinvertebrates (Gutt and Piepenburg, 2003). In the depth range we sampled, on the WAP the effects of iceberg scour have only been studied quantitatively at Rothera Station, although efforts are being made to expand this work to other areas (Deregibus et al., 2017). Iceberg scour at Rothera dramatically decreases with depth between 10 m and 40 m (Robinson et al., 2021), and about a quarter of the benthos is ice-scoured in most years with higher rates in some years (Barnes et al., 2014). Although benthic communities can recover from ice scour

disturbance within 10 years, they are likely in continual successional stages of recovery (Zwerschke et al., 2021).

The depth distributions of both fleshy macroalgae and macroinvertebrates at many of our study sites suggest effects from ice scour. For example, the lack of overstory brown macroalgae above 20 m at site D in the Wauwermans Islands seems very likely to be due to widespread iceberg scour within the previous few years, with sufficient time for smaller, red macroalgae to recover or recolonize but not sufficient time for the growth of overstory browns. From site G southward there was a general pattern of increasing fleshy macroalgal cover as depth increased, although this relationship was statistically significant only in vertical transect intervals at site L. At many of these sites, fleshy macroalgal cover peaked at intermediate depths. The increased cover with depth at these southern sites would be consistent with a greater impact from ice scour in the shallows than at most of the more northerly sites. The decreased fleshy macroalgal cover at the greatest depths, where it occurred, was perhaps attributable to decreasing irradiance. Iceberg scour can also have major impacts in the Arctic that decrease with depth. Heine (1989) observed severe iceberg impacts on benthic macroalgae and macroinvertebrates in exposed areas to 12 m depth but not deeper or in shallower depressions that protected the flora and fauna in the Bering Sea. Conlan et al. (1998) reported that ice scour decreased dramatically between 0 m and 30 m at two of three Arctic sites with no scour occurring at any of the three below 30 m. Filbee-Dexter et al. (2022) reported increases in kelp cover between 5 m and 15 m depths across many of 55 sites in the Canadian Arctic, which they attributed to decreases in ice scour or freshwater input.

4.3. Relationships between ice cover, macroalgae, and macroinvertebrates

As noted previously, we had no a priori reason to choose any of the available sea ice metric datasets for comparison with percent cover of the benthic organisms, nor to choose annual versus summer-only data. Consequently, we performed correlation analyses with both annual and summer ice concentrations from all four datasets. In every case, fleshy macroalgal cover was strongly, negatively correlated to sea ice cover. With the National Ice Center and AMSR2 Bootstrap ice datasets, the correlations were slightly stronger with log-transformed macroalgal cover data, so we reported correlations for both untransformed and log-transformed macroalgal covers for all ice datasets. Although ice cover generally increased to the south, sites in the northern half of the study area such as G and I, which had sea ice concentrations comparable to those in the southern half in the National Ice Center dataset and both AMSR2 datasets, also had levels of fleshy macroalgal cover that were more comparable to the southern sites than the northern sites with lower ice cover. Together, these observations clearly support our hypothesis (and that of Moe and DeLaca, 1976) that sea ice cover is a main driver influencing fleshy macroalgal abundance in this portion of the WAP. Strong negative correlations between sea ice cover and fleshy macroalgal cover have also been

reported from several areas in East Antarctica (Clark et al., 2013; Clark et al., 2015a; Michel et al., 2019) and in the Arctic (Scherrer et al., 2019; Goldsmit et al., 2021; Filbee-Dexter et al., 2022; Wiktor et al., 2022). Solar insolation obviously also decreases southward. To calculate the difference over our study area, average global horizontal solar irradiance was modeled over an entire year using the r.sun module in Grass GIS (Hofierka and Šúri, 2002). The model accounted for topographic shading but assumed a uniform Linke Atmospheric turbidity factor, for example, variations in cloud cover were not considered. The average daily horizontal daily solar irradiance was found to vary by 9.91% among sites (from 3.52 to 3.90 KWh m⁻² day⁻¹), which is considerably less than the relative difference in sea ice cover over our study area.

Although there were no significant correlations of macroinvertebrate cover with any of the sea ice datasets or fleshy macroalgal cover, macroinvertebrate Shannon diversity was positively correlated with most of the sea ice cover datasets. However, there may be an indirect basis for this correlation. Macroinvertebrate Shannon diversity correlated negatively with fleshy macroalgal cover, which as noted is strongly negatively correlated with sea ice cover. Macroinvertebrate diversity seems much more likely to be influenced by macroalgal diversity than by sea ice, even though the percent cover of macroinvertebrates was not correlated with fleshy macroalgal cover. For example, some macroinvertebrate species may be better or worse as competitors with macroalgae. Macroinvertebrate species richness also correlated negatively with fleshy macroalgal cover, although not significantly with sea ice cover. Patterns for the total community, however, were opposite of those for macroinvertebrates alone. Overall community Shannon diversity and species richness were both negatively correlated with sea ice cover and positively correlated with fleshy macroalgal percent cover. This apparent greater contribution of fleshy macroalgae to community diversity cannot be attributed simply to more macroalgal categories being included in the analysis, as the number of macroalgal categories and macroinvertebrate categories was almost equal (Table S2).

Our results differ in many ways from observations and predictions from studies of nine sites with varying annual sea ice cover in bays of the Windmill Islands (66°S in East Antarctica) reported by Clark et al. (2013), which were subsequently extrapolated to other regions of Antarctica (Clark et al., 2015b). As in the present study, these investigators also observed strong inverse correlations between annual sea ice cover and both macroalgal abundance and species richness, but they observed positive correlations between sea ice cover and macroinvertebrate cover, particularly if two very abundant species (the bryozoan *Inversiula nutrix* and the polychaete *Spirorbis nordenskjoldi*) were not included in the analysis (Clark et al., 2013). They also reported a significant positive correlation between sea ice cover and macroinvertebrate species richness. In addition, Clark et al. (2013) measured the underwater light levels at their nine sites along with the light requirements for growth in the only four common macroalgae (*Desmarestia menziesii*, *Himantothallus grandifolius*,

Iridaea cordata, and *Palmaria decipiens*). Based upon those results, they modeled the impact of increased irradiance due to earlier annual sea ice retreat and predicted that even relatively modest decreases in ice cover could push communities at sites currently dominated by benthic macroinvertebrates across a “tipping point” to macroalgal dominance. They predicted that resultant communities would have overall lower species richness than present in higher ice cover, invertebrate dominated communities (Clark et al., 2013).

The difference in conclusions about overall community species richness between the present study and that of Clark et al. (2013) in the Windmill Islands is likely due, at least in part, to the presence of very different macroalgal communities. Clark et al. (2013) reported 36 species of macroinvertebrates but apparently (based on their graphs) only five total fleshy macroalgal species. If an increase in the abundance of those species would replace some of the macroinvertebrate species instead of providing additional habitat and food, then increasing macroalgal dominance could decrease overall species richness. However, nothing in any of our data on macroalgal or macroinvertebrate percent cover, Shannon diversity, or species richness along the sea ice cover gradient present across our WAP sites is consistent with the existence of a narrow tipping point where a small change in ice cover would result in a dramatic shift from macroinvertebrate to macroalgal cover or to a shift in community diversity. Where significant changes correlated to sea ice cover were observed, the relationships were linear (including with untransformed data where correlations were slightly stronger with log-transformed data). Perhaps the more diverse macroalgal assemblages in the WAP provide a greater spectrum of physiological or morphological characteristics that in some way provide benefits to the macroinvertebrate assemblages that do not occur to the same extent in the less macroalgal-diverse East Antarctica communities.

With respect to overall community diversity, neither the present study nor those of Clark et al. (2013, 2015b, 2017) accurately enumerate the total invertebrate assemblages and certainly on the WAP—probably also elsewhere in Antarctica—vastly underreport invertebrate species richness and the numbers of individuals by not including mesoinvertebrates, particularly those associated with fleshy macroalgae. Amphipods and small gastropods are both species-rich and abundant on WAP macroalgae, and both are thought to be important mutualists with their macroalgal hosts, reducing biofouling on the hosts by consuming microalgal and filamentous macroalgal epiphytes (Amsler et al., 2012b, 2014, 2019). Mesoinvertebrates are much too small to be visible in our video recordings and apparently were also not enumerated in the East Antarctica studies. Past studies near Palmer Station have identified 32 taxa of gammaridean amphipods (most identified to species level but some taxa including multiple species) associated with eight common macroalgal species (Huang et al., 2007; Aumack et al., 2011). They are particularly abundant on branched macroalgae such as *Desmarestia menziesii*, *D. anceps*, and *Plocamium* sp. with

densities ranging from approximately 2 to 20 amphipods g^{-1} wet weight alga (Huang et al., 2007). When combined with raw macroalgal biomass m^{-2} data from Amsler et al. (1995) these densities extrapolate to 26,000 to 308,000 amphipods m^{-2} of the benthos in solid stands of the host macroalgae (Amsler et al., 2008). Similar high densities have been reported for *D. anceps* from Signy Island (60°S latitude) by Richardson (1977). Amphipods also associate with macroinvertebrates, and Amsler et al. (2009) reported 38 amphipod species in association with 20 species of sponges near Palmer Station. Although the way amphipod densities were normalized (macroalgal weight vs. total sponge volume) makes the studies not directly comparable, amphipods are clearly much less abundant on sponges than on branched macroalgae. Small gastropods are also abundant on macroalgae (Amsler et al., 2015; Amsler et al., 2022). Amsler et al. (2022) reported 35 gastropod species associated with five macroalgal species at Palmer Station. Although many other reports of gastropod species numbers along the WAP based on different collection methods are lower, WAP macroalgae probably commonly support relatively high numbers of gastropod species (Amsler et al., 2022). Clearly, the present and prior studies (e.g., Clark et al., 2013; Clark et al., 2015b; Clark et al., 2017), where methodological limitations have prevented the inclusion of smaller, motile invertebrates, are missing important members of the communities. Future studies of the influence of sea ice or other abiotic (or biotic) parameters on the Antarctic benthos would be improved by incorporating additional methods to enable their inclusion.

4.4. Percent cover versus biomass

The video transect methodology we employed requires extensive post-sampling analysis (e.g., in the present study analysis of 107,000 random points from 2,140 individual images, which took many person-months) but enables relatively rapid sampling with respect to time spent underwater and to total time spent in the field. Those aspects are particularly advantageous when working from oceanographic vessels that are expensive to operate and/or in polar regions where water temperatures near and below 0°C severely limit the duration of scuba dives. Both of those were true of the present study, with the additional temporal limitation of short daylengths during April and May in our high latitude, southern hemisphere study area. However, the percent cover data generated are not directly relatable to total biomass, which is the parameter most relevant for understanding macroalgal inputs into food webs and for estimating potential blue carbon contributions.

Further complicating such an effort for the communities studied here, conversion factors between macroalgal cover and biomass would vary greatly between taxa and, for some taxa, between sampling locations. This variability is particularly true for the overstory brown macroalgae and especially for *Desmarestia menziesii* and *D. anceps*, which usually dominate in shallower waters in the northern WAP. These species can be up to 3 m to 4 m in length, respectively, with multiple orders of branching (Wiencke

and Clayton, 2002), often rising a meter or more off the bottom (authors' personal observations). Consequently, a random video analysis point falling on one of these huge thalli would represent many-fold more actual biomass from multiple layers present underneath that point than a point falling on one of the much smaller understory red macroalgae. This effect would be less so for the overstory brown *Himantothallus grandifolius*, which forms large blades that lie decumbent on the bottom. Individuals have one to a few blades that can be up to 17 m in length and nearly a meter in width (Dieckmann et al., 1985). These thick blades often overlap along their edges and, in dense stands, can have up to several blades from one or more individuals completely overlapping. Consequently, they probably still represent more biomass per point in video analysis than most understory red macroalgae, but not to the extent of the densely branched *Desmarestia* spp. To illustrate this consequence, although the brown macroalgae contributed much and often most of the percent cover at most of our more northern study sites, this contribution is much lower than the relative contribution of brown macroalgae to total biomass in two previous studies at Palmer Station. There the overstory browns contributed approximately 80% to over 95% of the total macroalgal biomass at depths below 5 m depth (DeLaca and Lipps, 1976; Amsler et al., 1995).

However, were one to calculate conversion factors between percent cover and biomass from the northern sites such as those around Palmer Station, both the absolute factors for *Desmarestia* spp. and their values relative to red macroalgae would certainly be different at the southernmost of our sample sites. Although *Desmarestia menziesii* was present at all sites except for K, individuals at the southern sites were much smaller and rarely overlapped. Unlike *D. menziesii* from more northern sites, a point in a percent cover analysis falling on part of a thallus would thus have at most only a few additional thallus layers beneath contributing biomass. With *Himantothallus grandifolius*, smaller individuals and lower overall cover would rarely result in overlapping blades also probably necessitating different cover-to-biomass conversion factors. Making full use of these kinds of video data, which can be gathered relatively quickly in the field, for applications where standing biomass (and often its turnover) is what one truly desires to understand, would require developing conversions for different taxa or functional groups at multiple sites throughout the latitudinal range.

4.5. Extrapolations to past and future macroalgal assemblages

Our data represent a temporal snapshot recorded over 25 days in 2019 from communities at 14 sites spread over a 450 km latitudinal study area. Ideally projections through time should be based on data with much greater temporal replication so as to better incorporate all aspects of interannual variation. However, this snapshot, which is all that we presently have, represents the most comprehensive data on this system to date, given the difficulties of accessing the remote areas of the WAP. With the strong correlation that we observed between sea ice cover and

macroalgal cover, including to the Sea Ice Index dataset that goes back 40 years, and with the large declines in Antarctic sea ice cover predicted for the future, we believe that considering hindcasts and forecasts even based on a single snapshot of data from 2019 is constructive. We view this approach as providing a coarse indication of how communities may have been changing in the recent past and of how they may change in the future. We put little confidence in the specific macroalgal covers projected, and recognize that some are clearly exaggerated and/or improbable, and that some are impossible.

The highest overall macroalgal cover observed was 79.7%. Although percent cover can approach 100% at some depths in individual transects, periodic iceberg scour is probably a constant phenomenon, reducing benthic cover. Ice-scouring may prevent communities from ever reaching climax stages of 100% macroalgal cover, and we have no evidence (or personal observations) that at the level of an entire site, macroalgal cover could exceed 80% by much. Consequently, we believe the hindcast projections much above 80% from the high macroalgal cover sites could be unrealistic. Applying that limit, the high macroalgal cover sites would be projected to have changed little since the late 1980s. That projection is consistent with our (C. Amsler) personal, subjective observations at Palmer Station from 1989 and multiple years since 2000 that while individual species may vary, the overall macroalgal cover has remained relatively constant.

Hindcast projections for the other, moderate-to-high ice cover sites show dramatic variation, particularly over the most recent 15 years. While the huge, rapid changes in macroalgal cover projected are quite improbable, and the negative covers predicted for some sites and years are impossible, concluding that significant changes could have been occurring at some of these sites over the period of satellite sea ice records is reasonable. At sites with currently low macroalgal cover and macroalgal species richness, particularly site K that had no fleshy macroalgae in 2019, any increase in macroalgal cover would likely depend on the new recruitment of additional macroalgal species beyond the currently nearly ubiquitous *Desmarestia menziesii*. A majority of the sites (A through H and J), however, did not differ statistically in macroalgal assemblage similarity in 2019. Although the magnitude of the projected changes at the lower ice sites in that group are also almost certainly unrealistic, more modest but still substantial increases in macroalgal cover would not have required immigration of additional species.

Most sea ice models have predicted that Antarctic sea ice extent should have been declining over recent decades, but this decline has not happened for the continental area as a whole (Stammerjohn and Maksym, 2017; Maksym, 2019; Eays et al., 2021; Blanchard-Wrigglesworth et al., 2022) nor consistently in our study area (Figures S10 and S11). The discrepancy may be because in the past models have not adequately incorporated wind-driven ice movements or sea surface temperature changes (Blanchard-Wrigglesworth et al., 2022). Nevertheless, a variety of models predict that annual sea ice cover off the Antarctic continent as a whole will decline 15% to 50% or more by

2100 (Cavanagh et al., 2017; Roach et al., 2020; Rackow et al., 2022). Understanding how such changes could affect benthic macroalgae is critical for understanding how benthic communities overall may change, and for understanding future macroalgal contributions to projections of Antarctic blue carbon. The projections we report for future fleshy macroalgal percent cover are subject to all the caveats just discussed for hindcast projections. We have performed these projections with the three best correlations, which were also from the three different satellite ice data products, and again assumed that fleshy macroalgal cover cannot substantially exceed 80% for an entire site. There is considerable variation between the three projections at individual sites. Using the lowest projection from the three regressions for each individual site and sea ice percent reduction, there are only small projected changes for the northern sites which already have macroalgal cover approaching 80%. However, the projected increases at sites that currently have high ice cover and low macroalgal cover are substantial, often even with only a 15% decrease in sea ice. As described for hindcast predictions, increases in macroalgal cover at low macroalgal cover but high diversity sites such as G and J might not require recruitment of additional macroalgal species. However, as the projected sea ice changes are for the next three-quarters of the century, we find it reasonable to postulate that the macroalgal flora represented in the northern part of our study area (and northward from it throughout the WAP) would have time to spread farther south and potentially continue expanding throughout much of the rest of the Antarctic coastline.

Migration of the northern WAP flora farther south into our study area and beyond assumes that total annual irradiance is the main constraint limiting macroalgal distribution. That assumption may not be true of the overstory brown alga *Desmarestia anceps*, where southward range expansion may be limited by the light requirements of its reproductive stages. The only previous reports of *D. anceps* south of Palmer Station are Heiser et al. (2023) from the Wauwermans Islands near our site D and a brief mention of it being collected in southern Marguerite Bay near our site N sometime between 1947 and 1981 (Etcheverry, 1983). There is a juvenile form of *D. menziesii* that resembles *D. anceps*, which was only recently described in the literature, although it was represented in herbarium specimens collected previously (Küpper et al., 2019), and even adult forms can sometimes be difficult to distinguish without examining holdfast morphology. It seems likely that the Etcheverry (1983) southern Marguerite Bay report may actually represent *D. menziesii*, and our report of *D. anceps* at site G may represent the southernmost record of this species. At site G, it was recorded only from a single depth (15 m) on a single transect, with *D. menziesii* being much more widespread across depths and transects.

Wiencke et al. (1996) hypothesized that the southern distribution limit of *Desmarestia anceps* could be determined by daylength requirements of the (essentially) microscopic, filamentous gametophyte stage. Under otherwise growth-promoting culture conditions, both male and female gametophytes required short days for gametogenesis, with males

only becoming fertile after 6 weeks or more at daylengths of 5–7 hours (next shorter and longer daylengths tested were 3 and 9 hours; Wiencke et al., 1996). Although such short daylengths certainly occur throughout our study area, daylengths change progressively more rapidly to the south. Based on meteorological tables, Wiencke et al. (1996) reported that daylengths in this range only occur for a few weeks south of approximately 65°S latitude. That period of time would not be sufficient within the narrow, required range of 5–7 hours daylengths for *D. anceps* gametophytes to complete gametogenesis. Similar daylength constraints are unlikely in gametophytes of the other members of the Desmarestiaceae that we observed (Wiencke and Clayton, 1990; Wiencke et al., 1991; Wiencke et al., 1995; Matula et al., 2022).

The nearly complete disappearance of *Desmarestia anceps* just tens of kilometers south of Palmer Station where it commonly dominates the flora is certainly consistent with the hypothesis of Wiencke et al. (1996) that its distribution is limited by daylength. At sites without *D. anceps* we found *D. menziesii* throughout the depth range commonly dominated by *D. anceps* in the northern WAP, but the largest *D. menziesii* individuals are considerably smaller than the largest *D. anceps*. Although *D. menziesii* might fill the depth range of *D. anceps* as sea ice is reduced in the future and contribute similar percent cover in these southerly areas, it could not likely make as great a biomass contribution as *D. anceps* does in the northern WAP.

5. Conclusions

As we hypothesized, sea ice cover, which reduces light penetration to the benthos, is a major factor influencing the percent cover of fleshy macroalgae across our study sites in the central WAP. Consequently, predicted future decreases in sea ice cover due to climate change will likely lead to substantial increases in macroalgal cover in areas where ice cover is currently relatively high and macroalgal cover is low to moderate. Decreasing ice cover should greatly increase macroalgal contributions to future blue carbon sequestration. Climate change has also accelerated glacier retreat, however, which can decrease light available to benthic macroalgae due to increased sediment runoff, particularly in nearby bays, but over longer periods this retreat uncovers new benthic habitats suitable for macroalgal colonization (Quartino et al., 2013; Sahade et al., 2015; Quartino et al., 2020). Although the overall net impacts of the changing global climate on WAP macroalgae and on their contribution to blue carbon are likely to be positive, they will vary over space and time.

As decreases in sea ice lead to increased macroalgal biomass, the concomitant increase in macroalgal carbon availability is likely to alter benthic food webs, although understanding details of how and to what extent await further study. While overall macroinvertebrate cover did not correlate with either sea ice cover or fleshy macroalgal cover, increasing macroalgal cover did significantly decrease macroinvertebrate diversity and species richness even while increasing overall community diversity and species richness. Why this decrease occurs and how it impacts community dynamics also await further research. Future research

should also include mesoinvertebrates, which are known to be diverse, numerous, and functionally important members of macroalgal-dominated communities along the northern WAP. Increases in macroalgal cover under future sea ice conditions are certain to dramatically increase the numbers of mesoinvertebrates in the communities, although whether this increase will change their diversity and resilience remains to be determined.

Data accessibility statement

Data from the overall project including sea ice concentration data are available at the United States Antarctic Program Data Center (<https://www.usap-dc.org/view/project/p0010104>). These include the original underwater videos analyzed, which are available through <https://doi.org/10.15784/601610>, and the raw percent cover data from the video analysis compiled from Coral Point Count with Excel extensions, which are available at <https://doi.org/10.15784/601619>.

Supplemental files

The supplemental files for this article can be found as follows:

Appendices S1–S3, Figures S1–S12, Tables S1–S14.

Acknowledgments

This study would not have been possible without our shipmates on the ARSV *Laurence M. Gould* (LMG). They included Captain Zsolt Esztergomi and his LMG crew and the Antarctic Support Contract LMG team of Sean Bercaw, Chuck Holloway, Linnah Neidel, Kevin Pedigo, Gina Pikton, and Rich Thompson. We are also grateful to Dr. Chris Mah for assistance with echinoderm identification and to two anonymous reviewers for constructive comments that improved the final version of the manuscript.

Funding

The project was funded by National Science Foundation awards ANT-1744550 (CDA, JBM), ANT-1744584 (AGK), ANT-1744570 (AWEG), and ANT-1744602 (KI) from the Antarctic Organisms and Ecosystems Program. JBM acknowledges the support of an Endowed University Professorship in Polar and Marine Biology provided by the University of Alabama at Birmingham.

Competing interests

The authors declare no competing interests.

Author contributions

Contributed to conception and design: CDA, AGK, AWEG, KI, JBM.

Contributed to acquisition of data: CDA, MOA, AGK, AWEG, KI, SH, ATL, JBS, RW.

Contributed to analysis and interpretation of data: CDA, MOA, AGK, KI.

Drafted and/or revised the article: CDA, MOA, AGK, AWEG, KI, JBM, SH, ATL, JBS, RW.

Approved the submitted version for publication: CDA, MOA, AGK, AWEG, KI, JBM, SH, ATL, JBS, RW.

References

- Amsler, CD, Amsler, MO, Curtis, MD, McClintock, JB, Baker, BJ.** 2019. Impacts of gastropods on epiphytic microalgae on the brown macroalga *Himantothallus grandifolius*. *Antarctic Science* **31**(2): 89–97. DOI: <http://dx.doi.org/10.1017/S0954102019000014>.
- Amsler, CD, Laur, DR, Quetin, LB, Rowley, RJ, Ross, RM, Neushul, M.** 1990. Quantitative analysis of the vertical distribution of overstory macroalgae near Anvers Island, Antarctica. *Antarctic Journal of the United States* **25**: 201–202.
- Amsler, CD, McClintock, JB, Baker, BJ.** 2008. Macroalgal chemical defenses in polar marine communities, in Amsler, CD ed., *Algal chemical ecology*. Berlin, Heidelberg: Springer-Verlag: 91–103.
- Amsler, CD, McClintock, JB, Baker, BJ.** 2012a. Palatability of living and dead detached Antarctic macroalgae to consumers. *Antarctic Science* **24**(6): 589–590. DOI: <http://dx.doi.org/10.1017/S0954102012000624>.
- Amsler, CD, McClintock, JB, Baker, BJ.** 2012b. Amphipods exclude filamentous algae from the Western Antarctic Peninsula benthos: Experimental evidence. *Polar Biology* **35**(2): 171–177. DOI: <http://dx.doi.org/10.1007/s00300-011-1049-3>.
- Amsler, CD, McClintock, JB, Baker, BJ.** 2014. Chemical mediation of mutualistic interactions between macroalgae and mesograzers structure unique coastal communities along the western Antarctic Peninsula. *Journal of Phycology* **50**(1): 1–10. DOI: <http://dx.doi.org/10.1111/jpy.12137>.
- Amsler, CD, McClintock, JB, Baker, BJ.** 2020. Chemical mediation of Antarctic macroalga-grazer interactions, in Gómez, I, Huovinen, P eds., *Antarctic seaweeds: Diversity, adaptation and ecosystem services*. Cham, Switzerland: Springer International Publishing: 339–363.
- Amsler, CD, Miller, LR, Edwards, RA, Amsler, MO, Engl, W, McClintock, JB, Baker, BJ.** 2022. Gastropod assemblages associated with *Himantothallus grandifolius*, *Sarcopeltis antarctica* and other subtidal macroalgae. *Antarctic Science* **34**(3): 246–255. DOI: <http://dx.doi.org/10.1017/S0954102022000153>.
- Amsler, CD, Rowley, RJ, Laur, DR, Quetin, LB, Ross, RM.** 1995. Vertical distribution of Antarctic Peninsular macroalgae: Cover, biomass, and species composition. *Phycologia* **34**(5): 424–430. DOI: <http://dx.doi.org/10.2216/i0031-8884-34-5-424.1>.
- Amsler, MO, Amsler, CD, von Salm, JL, Aumack, CF, McClintock, JB, Young, RM, Baker, BJ.** 2013. Tolerance and sequestration of macroalgal chemical defenses by an Antarctic amphipod: A “cheater” among mutualists. *Marine Ecology Progress Series* **490**: 79–90. DOI: <http://dx.doi.org/10.3354/meps10446>.
- Amsler, MO, Huang, YM, Engl, W, McClintock, JB, Amsler, CD.** 2015. Abundance and diversity of gastropods associated with dominant subtidal macroalgae from the western Antarctic Peninsula. *Polar Biology* **38**(8): 1171–1181. DOI: <http://dx.doi.org/10.1007/s00300-015-1681-4>.
- Amsler, MO, McClintock, JB, Amsler, CD, Angus, RA, Baker, BJ.** 2009. An evaluation of sponge-associated amphipods from the Antarctic Peninsula. *Antarctic Science* **21**: 579–589. DOI: <http://dx.doi.org/10.1017/S0954102009990356>.
- Andrade, C, Ríos, C, Gerdes, D, Brey, T.** 2016. Trophic structure of shallow-water benthic communities in the sub-Antarctic Strait of Magellan. *Polar Biology* **39**(12): 2281–2297. DOI: <http://dx.doi.org/10.1007/s00300-016-1895-0>.
- Arnaud, PM, Jażdewski, K, Presler, P, Siciński, J.** 1986. Preliminary survey of benthic invertebrates collected by Polish Antarctic Expeditions in Admiralty Bay (King George Island, South Shetland Islands, Antarctica). *Polish Polar Research* **7**(1–2): 7–24.
- Aromokeye, DA, Willis-Poratti, G, Wunder, LC, Yin, X, Wendt, J, Richter-Heitmann, T, Henkel, S, Vázquez, S, Elvert, M, Mac Cormack, W, Friedrich, MW.** 2021. Macroalgae degradation promotes microbial iron reduction via electron shuttling in coastal Antarctic sediments. *Environment International* **156**: 106602. DOI: <http://dx.doi.org/10.1016/j.envint.2021.106602>.
- Aumack, CF, Amsler, CD, McClintock, JB, Baker, BJ.** 2011. Changes in amphipod densities among macroalgal habitats in day versus night collections along the Western Antarctic Peninsula. *Marine Biology* **158**: 1879–1885. DOI: <http://dx.doi.org/10.1007/s00227-011-1700-0>.
- Aumack, CF, Lowe, AT, Amsler, CD, Amsler, MO, McClintock, JB, Baker, BJ.** 2017. Gut content, fatty acid, and stable isotope analyses reveal dietary sources of macroalgal-associated amphipods along the western Antarctic Peninsula. *Polar Biology* **40**: 1371–1384. DOI: <http://dx.doi.org/10.1007/s00300-016-2061-4>.
- Barnes, DKA, Brockington, S.** 2003. Zoobenthic biodiversity, biomass and abundance at Adelaide Island, Antarctica. *Marine Ecology Progress Series* **249**: 145–155. DOI: <http://dx.doi.org/10.3354/meps249145>.
- Barnes, DKA, Fenton, M, Cordingley, A.** 2014. Climate-linked iceberg activity massively reduces spatial competition in Antarctic shallow waters. *Current Biology* **24**(12): R553–R554. DOI: <http://dx.doi.org/10.1016/j.cub.2014.04.040>.
- Barnes, DKA, Fleming, A, Sands, CJ, Quartino, ML, Deregiibus, D.** 2018. Icebergs, sea ice, blue carbon and Antarctic climate feedbacks. *Philosophical Transactions of the Royal Society A: Mathematical, Physical and Engineering Sciences* **376**(2122): 20170176. DOI: <http://dx.doi.org/10.1098/rsta.2017.0176>.
- Barnes, DKA, Sands, CJ, Paulsen, ML, Moreno, B, Moreau, C, Held, C, Downey, R, Bax, N, Stark, JS, Zwerschke, N.** 2021. Societal importance of Antarctic negative feedbacks on climate change: Blue carbon gains from sea ice, ice shelf and glacier losses.

- The Science of Nature* **108**(5): 43. DOI: <http://dx.doi.org/10.1007/s00114-021-01748-8>.
- Bax, N, Sands, CJ, Gogarty, B, Downey, RV, Moreau, CVE, Moreno, B, Held, C, Paulsen, ML, McGee, J, Haward, M, Barnes, DKA.** 2021. Perspective: Increasing blue carbon around Antarctica is an ecosystem service of considerable societal and economic value worth protecting. *Global Change Biology* **27**(1): 5–12. DOI: <http://dx.doi.org/10.1111/gcb.15392>.
- Becker, S, Quartino, ML, Campana, GL, Bucolo, P, Wiencke, C, Bischof, K.** 2011. The biology of an Antarctic rhodophyte, *Palmaria decipiens*: Recent advances. *Antarctic Science* **23**(5): 419–430. DOI: <http://dx.doi.org/10.1017/S0954102011000575>.
- Benson, BL.** 1989. Airlift sampler: Applications for hard substrata. *Bulletin of Marine Science* **44**(2): 752–756.
- Bindschadler, R, Vornberger, P, Fleming, A, Fox, A, Mullins, J, Binnie, D, Paulsen, SJ, Granneman, B, Gorodetzky, D.** 2008. The Landsat image mosaic of Antarctica. *Remote Sensing of Environment* **112**(12): 4214–4226. DOI: <http://dx.doi.org/10.1016/j.rse.2008.07.006>.
- Blanchard-Wrigglesworth, E, Eisenman, I, Zhang, S, Sun, S, Donohoe, A.** 2022. New perspectives on the enigma of expanding Antarctic sea ice. *Eos* **103**. DOI: <http://dx.doi.org/10.1029/2022EO220076>.
- Bowden, DA.** 2005. Quantitative characterization of shallow marine benthic assemblages at Ryder Bay, Adelaide Island, Antarctica. *Marine Biology* **146**(6): 1235–1249. DOI: <http://dx.doi.org/10.1007/s00227-004-1526-0>.
- Braeckman, U, Pasotti, F, Vázquez, S, Zacher, K, Hoffmann, R, Elvert, M, Marchant, H, Buckner, C, Quartino, ML, Mác Cormack, W, Soetaert, K, Wenzhöfer, F, Vanreusel, A.** 2019. Degradation of macroalgal detritus in shallow coastal Antarctic sediments. *Limnology and Oceanography* **64**: 1423–1441. DOI: <http://dx.doi.org/10.1002/lno.11125>.
- Brêthes, JC, Ferreyra, G, de la Vega, S.** 1994. Distribution, growth and reproduction of the limpet *Nacella (Patinigera) concinna* (Strebel 1908) in relation to potential food availability in Esperanza Bay (Antarctic Peninsula). *Polar Biology* **14**(3): 161–170. DOI: <http://dx.doi.org/10.1007/BF00240521>.
- Brouwer, PEM.** 1996a. Decomposition in situ of the sublittoral Antarctic macroalga *Desmarestia anceps* Montagne. *Polar Biology* **16**(2): 129–137. DOI: <http://dx.doi.org/10.1007/BF02390433>.
- Brouwer, PEM.** 1996b. In situ photosynthesis and estimated annual production of the red macroalga *Myriogramme mangini* in relation to underwater irradiance at Signy Island (Antarctica). *Antarctic Science* **8**(3): 245–252. DOI: <http://dx.doi.org/10.1017/S095410209600034X>.
- Buchholz, CM, Wiencke, C.** 2016. Working on a baseline for the Kongsfjorden food web: Production and properties of macroalgal particulate organic matter (POM). *Polar Biology* **39**(11): 2053–2064. DOI: <http://dx.doi.org/10.1007/s00300-015-1828-3>.
- Cárdenas, CA, Newcombe, EM, Hajdu, E, Gonzalez-Aravena, M, Geange, SW, Bell, JJ.** 2016. Sponge richness on algae-dominated rocky reefs in the western Antarctic Peninsula and the Magellan Strait. *Polar Research* **35**(1): 30532. DOI: <http://dx.doi.org/10.3402/polar.v35.30532>.
- Cavanagh, RD, Murphy, EJ, Bracegirdle, TJ, Turner, J, Knowland, CA, Corney, SP, Smith, WO, Waluda, CM, Johnston, NM, Bellerby, RGJ, Constable, AJ, Costa, DP, Hofmann, EE, Jackson, JA, Staniland, IJ, Wolf-Gladrow, D, Xavier, JC.** 2017. A synergistic approach for evaluating climate model output for ecological applications. *Frontiers in Marine Science* **4**: 308. DOI: <http://dx.doi.org/10.3389/fmars.2017.00308>.
- Clark, GF, Marzinelli, EM, Fogwill, JC, Turney, MCS, Johnston, EL.** 2015a. Effects of sea-ice cover on marine benthic communities: A natural experiment in Commonwealth Bay, East Antarctica. *Polar Biology* **38**(8): 1213–1222. DOI: <http://dx.doi.org/10.1007/s00300-015-1688-x>.
- Clark, GF, Raymond, B, Riddle, MJ, Stark, JS, Johnston, EL.** 2015b. Vulnerability of Antarctic shallow invertebrate-dominated ecosystems. *Austral Ecology* **40**(4): 482–491. DOI: <http://dx.doi.org/10.1111/aec.12237>.
- Clark, GF, Stark, JS, Johnston, EL, Runcie, JW, Goldsworthy, PM, Raymond, B, Riddle, MJ.** 2013. Light-driven tipping points in polar ecosystems. *Global Change Biology* **19**(12): 3749–3761. DOI: <http://dx.doi.org/10.1111/gcb.12337>.
- Clark, GF, Stark, JS, Palmer, AS, Riddle, MJ, Johnston, EL.** 2017. The roles of sea-ice, light and sedimentation in structuring shallow Antarctic benthic communities. *PLoS One* **12**(1): e0168391. DOI: <http://dx.doi.org/10.1371/journal.pone.0168391>.
- Clarke, A, Murphy, EJ, Meredith, MP, King, JC, Peck, LS, Barnes, DKA, Smith, RC.** 2007. Climate change and the marine ecosystem of the western Antarctic Peninsula. *Philosophical Transactions of the Royal Society B-Biological Sciences* **362**(1477): 149–166. DOI: <http://dx.doi.org/10.1098/rstb.2006.1958>.
- Clarke, KR, Gorley, RN, Somerfield, PJ, Warwick, RM.** 2014. *Change in marine communities: An approach to statistical analysis and interpretation*. 3rd ed. Plymouth, UK: PRIMER-E.
- Conlan, KE, Lenihan, HS, Kvitek, RG, Oliver, JS.** 1998. Ice scour disturbance to benthic communities in the Canadian High Arctic. *Marine Ecology Progress Series* **166**: 1–16. DOI: <http://dx.doi.org/10.3354/meps166001>.
- Corbisier, TN, Petti, MAV, Skowronski, RSP, Brito, TAS.** 2004. Trophic relationships in the nearshore zone of Martel Inlet (King George Island, Antarctica): $\delta^{13}\text{C}$ stable-isotope analysis. *Polar Biology* **27**(2): 75–82. DOI: <http://dx.doi.org/10.1007/s00300-003-0567-z>.

- Dawson, R, Schramm, W, Bolter, M.** 1985. Factors influencing the production, decomposition and distribution of organic matter in Admiralty Bay, King George Island, in Seigfried, WR, Condy, PR, Laws, RM eds., *Antarctic nutrient cycles and food webs*. Berlin, Germany: Springer-Verlag: 109–114.
- Dedrick, KR, Partington, K, Van Woert, M, Bertoia, CA, Benner, D.** 2001. U.S. National/Naval Ice Center digital sea ice data and climatology. *Canadian Journal of Remote Sensing* **27**(5): 457–475. DOI: <http://dx.doi.org/10.1080/07038992.2001.10854887>.
- DeLaca, TE, Lipps, JH.** 1976. Shallow water marine associations, Antarctic Peninsula. *Antarctic Journal of the United States* **11**: 12–20.
- Deregibus, D, Quartino, ML, Zacher, K, Campana, GL, Barnes, DKA.** 2017. Understanding the link between sea ice, ice scour and Antarctic benthic biodiversity—The need for cross-station and international collaboration. *Polar Record* **53**(2): 143–152. DOI: <http://dx.doi.org/10.1017/S0032247416000875>.
- Deregibus, D, Zacher, K, Bartsch, I, Campana, GL, Momo, FR, Wiencke, C, Gómez, I, Quartino, ML.** 2020. Carbon balance under a changing light environment, in Gómez, I, Huovinen, P eds., *Antarctic seaweeds: Diversity, adaptation and ecosystem services*. Cham, Switzerland: Springer International Publishing: 173–191.
- Dhargalkar, VK, Burton, HR, Kirkwood, JM.** 1988. Animal associations with the dominant species of shallow water macrophytes along the coastline of the Vestfold Hills, Antarctica. *Hydrobiologia* **165**: 141–150.
- Dieckmann, G, Reichardt, W, Zieliński, D.** 1985. Growth and production of the seaweed, *Himantothallus grandifolius*, at King George Island, in Siegfried, WR, Condy, P, Laws, RM eds., *Antarctic nutrient cycles and food webs*. Berlin, Germany: Springer-Verlag: 104–108.
- Dolliver, J, O'Connor, N.** 2022. Whole system analysis is required to determine the fate of macroalgal carbon: A systematic review. *Journal of Phycology* **58**(3): 364–376. DOI: <http://dx.doi.org/10.1111/jpy.13251>.
- Ducklow, HW, Baker, K, Martinson, DG, Quetin, LB, Ross, RM, Smith, RC, Stammerjohn, SE, Vernet, M, Fraser, W.** 2007. Marine pelagic ecosystems: The West Antarctic Peninsula. *Philosophical Transactions of the Royal Society B-Biological Sciences* **362**(1477): 67–94. DOI: <http://dx.doi.org/10.1098/rstb.2006.1955>.
- Ducklow, HW, Fraser, WR, Meredith, MP, Stammerjohn, SE, Doney, SC, Martinson, DG, Sailley, SF, Schofield, OM, Steinberg, DK, Venables, HJ, Amsler, CD.** 2013. West Antarctic Peninsula: An ice-dependent coastal marine ecosystem in transition. *Oceanography* **26**(3): 190–203. DOI: <http://dx.doi.org/10.5670/oceanog.2013.62>.
- Duggins, DO, Simenstad, C, Estes, J.** 1989. Magnification of secondary production by kelp detritus in coastal marine ecosystems. *Science* **245**: 170–173.
- Dunton, K.** 2001. $\delta^{15}\text{N}$ and $\delta^{13}\text{C}$ measurements of Antarctic Peninsula fauna: Trophic relationships and assimilation of benthic seaweeds. *American Zoologist* **41**: 99–112.
- Eayrs, C, Li, X, Raphael, MN, Holland, DM.** 2021. Rapid decline in Antarctic sea ice in recent years hints at future change. *Nature Geoscience* **14**(7): 460–464. DOI: <http://dx.doi.org/10.1038/s41561-021-00768-3>.
- Etcheverry, H.** 1983. Algas bentónicas de la Antártica Chilena. *Serie Científica INACH* **30**: 97–124.
- Falkowski, PG, Raven, JA.** 2007. *Aquatic photosynthesis*. 2nd ed. Princeton, NJ: Princeton University Press.
- Fetterer, F.** 2006. A selection of documentation related to National Ice Center Sea Ice Charts in Digital Format. National Snow and Ice Center Special Report #13. Available at https://nsidc.org/sites/nsidc.org/files/technical-references/nsidc_special_report_13.pdf. Accessed June 28, 2022.
- Fetterer, F, Knowles, K, Meier, WN, Savoie, M, Windnagel, AK.** 2017. Sea Ice Index, Version 3. [Antarctica]. Boulder, CO: NSIDC: National Snow and Ice Data Center, updated daily. DOI: <https://doi.org/10.7265/N5K072F8>. Accessed August 27, 2021.
- Field, CB, Behrenfeld, MJ, Randerson, JT, Falkowski, P.** 1998. Primary production of the biosphere: Integrating terrestrial and oceanic components. *Science* **281**(5374): 237–240. DOI: <http://dx.doi.org/10.1126/science.281.5374.237>.
- Filbee-Dexter, K, MacGregor, KA, Lavoie, C, Garrido, I, Goldsmit, J, Castro de la Guardia, L, Howland, KL, Johnson, LE, Konar, B, McKindsey, CW, Mundy, CJ, Schlegel, RW, Archambault, P.** 2022. Sea ice and substratum shape extensive kelp forests in the Canadian Arctic. *Frontiers in Marine Science* **9**: 754074. DOI: <http://dx.doi.org/10.3389/fmars.2022.754074>.
- Filbee-Dexter, K, Scheibling, RE.** 2014. Detrital kelp subsidy supports high reproductive condition of deep-living sea urchins in a sedimentary basin. *Aquatic Biology* **23**(1): 71–86. DOI: <http://dx.doi.org/10.3354/ab00607>.
- Fischer, G, Wiencke, C.** 1992. Stable carbon isotope composition, depth distribution and fate of macroalgae from the Antarctic Peninsula region. *Polar Biology* **12**: 341–348. DOI: <http://dx.doi.org/10.1007/BF00243105>.
- Gogarty, B, McGee, J, Barnes, DKA, Sands, CJ, Bax, N, Haward, M, Downey, R, Moreau, C, Moreno, B, Held, C, Paulsen, ML.** 2019. Protecting Antarctic blue carbon: As marine ice retreats can the law fill the gap? *Climate Policy* **20**(2): 1–14. DOI: <http://dx.doi.org/10.1080/14693062.2019.1694482>.
- Goldsmit, J, Schlegel, RW, Filbee-Dexter, K, MacGregor, KA, Johnson, LE, Mundy, CJ, Savoie, AM, McKindsey, CW, Howland, KL, Archambault, P.** 2021. Kelp in the eastern Canadian Arctic: Current and future predictions of habitat suitability and

- cover. *Frontiers in Marine Science* **8**: 742209. DOI: <http://dx.doi.org/10.3389/fmars.2021.742209>.
- Gómez, I, Huovinen, P.** 2020. Form and function in Antarctic seaweeds: Photobiological adaptations, zonation patterns, and ecosystem feedbacks, in Gómez, I, Huovinen, P eds., *Antarctic seaweeds: Diversity, adaptation and ecosystem services*. Cham, Switzerland: Springer International Publishing: 217–237.
- Gómez, I, Weykam, G, Klöser, H, Wiencke, C.** 1997. Photosynthetic light requirements, metabolic carbon balance and zonation of sublittoral macroalgae from King George Island (Antarctica). *Marine Ecology Progress Series* **148**: 281–293. DOI: <http://dx.doi.org/10.3354/meps148281>.
- Grange, LJ, Smith, CR.** 2013. Megafaunal communities in rapidly warming fjords along the west Antarctic Peninsula: Hotspots of abundance and beta diversity. *PLoS One* **8**(12): e77917. DOI: <http://dx.doi.org/10.1371/journal.pone.0077917>.
- Gutt, J, Piepenburg, D.** 2003. Scale-dependent impact on diversity of Antarctic benthos caused by grounding of icebergs. *Marine Ecology Progress Series* **253**: 77–83. DOI: <http://dx.doi.org/10.3354/meps253077>.
- Heine, JN.** 1989. Effects of ice scour on the structure of sublittoral marine algal assemblages of St. Lawrence and St. Matthew Islands, Alaska. *Marine Ecology Progress Series* **52**: 253–260.
- Heiser, S, Amsler, CD, McClintock, JB, Shilling, AJ, Baker, BJ.** 2020. Every rule has an exception: A cheater in the community-wide mutualism in Antarctic seaweed forests. *Integrative and Comparative Biology* **60**(6): 1358–1368. DOI: <http://dx.doi.org/10.1093/icb/icaa058>.
- Heiser, S, Shilling, AJ, Amsler, CD, McClintock, JB, Baker, BJ.** 2023. To change or not to change: Drivers of defensive secondary metabolite distribution in the red macroalga *Plocamium* sp. *Marine Biology* **170**(3): 31. DOI: <http://dx.doi.org/10.1007/s00227-023-04173-9>.
- Henley, SF, Schofield, OM, Hendry, KR, Schloss, IR, Steinberg, DK, Moffat, C, Peck, LS, Costa, DP, Bakker, DCE, Hughes, C, Rozema, PD, Ducklow, HW, Abele, D, Stefels, J, Van Leeuwe, MA, Brussaard, CPD, Buma, AGJ, Kohut, J, Sahade, R, Friedlaender, AS, Stammerjohn, SE, Venables, HJ, Meredith, MP.** 2019. Variability and change in the west Antarctic Peninsula marine system: Research priorities and opportunities. *Progress in Oceanography* **173**: 208–237. DOI: <http://dx.doi.org/10.1016/j.pocean.2019.03.003>.
- Hofierka, J, Sári, M.** 2002. The solar radiation model for open source GIS: Implementation and application, in *Proceedings of the open source GIS-GRASS users conference 2002*. Trento, Italy: Università degli studi di Trento.
- Huang, YM, Amsler, MO, McClintock, JB, Amsler, CD, Baker, BJ.** 2007. Patterns of gammaridean amphipod abundance and species composition associated with dominant sublittoral macroalgae along the western Antarctic Peninsula. *Polar Biology* **30**: 1417–1430. DOI: <http://dx.doi.org/10.1007/s00300-007-0303-1>.
- Huovinen, P, Gómez, I.** 2020. Underwater light environment of Antarctic seaweeds, in Gómez, I, Huovinen, P eds., *Antarctic seaweeds diversity, adaptation and ecosystem services*. Cham, Switzerland: Springer International Publishing: 131–153.
- Hurd, CL, Harrison, PJ, Bischof, K, Lobban, CS.** 2014. *Seaweed ecology and physiology. 2nd ed.* Cambridge, UK: Cambridge University Press.
- Irving, A, Connell, S, Johnston, E, Pile, A, Gillanders, B.** 2005. The response of encrusting coralline algae to canopy loss: An independent test of predictions on an Antarctic coast. *Marine Biology* **147**(5): 1075–1083.
- Johnston, E, Connell, S, Irving, A, Pile, A, Gillanders, B.** 2007. Antarctic patterns of shallow subtidal habitat and inhabitants in Wilke's Land. *Polar Biology* **30**(6): 781–788.
- Kaehler, S, Pakhomov, EA, Kalin, RM, Davis, S.** 2006. Trophic importance of kelp-derived suspended particulate matter in a through-flow sub-Antarctic system. *Marine Ecology Progress Series* **316**: 17–22. DOI: <http://dx.doi.org/10.3354/meps316017>.
- Kerr, R, Mata, MM, Mendes, CRB, Secchi, ER.** 2018. Northern Antarctic Peninsula: A marine climate hot-spot of rapid changes on ecosystems and ocean dynamics. *Deep Sea Research Part II: Topical Studies in Oceanography* **149**: 4–9. DOI: <http://dx.doi.org/10.1016/j.dsr2.2018.05.006>.
- Kirkwood, J, Burton, H.** 1988. Macrobenthic assemblages in Ellis Fjord, Vestfold Hills, Antarctica. *Marine Biology* **97**: 445–457.
- Knox, GA.** 2007. *The biology of the southern ocean. 2nd ed.* Boca Raton, FL: CRC Press.
- Kohler, KE, Gill, SM.** 2006. Coral Point Count with Excel extensions (CPCe): A Visual Basic program for the determination of coral and substrate coverage using random point count methodology. *Computers & Geosciences* **32**(9): 1259–1269. DOI: <http://dx.doi.org/10.1016/j.cageo.2005.11.009>.
- Krause-Jensen, D, Sejr, MK, Bruhn, A, Rasmussen, MB, Christensen, PB, Hansen, JLS, Duarte, CM, Bruntse, G, Wegeberg, S.** 2019. Deep penetration of kelps offshore along the west coast of Greenland. *Frontiers in Marine Science* **6**. DOI: <http://dx.doi.org/10.3389/fmars.2019.00375>.
- Küpper, FC, Amsler, CD, Morley, S, de Reviere, B, Reichardt, A, Peck, LS, Peters, AF.** 2019. Juvenile morphology of the large Antarctic canopy-forming brown alga, *Desmarestia menziesii* J. Agardh. *Polar Biology* **42**(11): 2097–2103. DOI: <http://dx.doi.org/10.1007/s00300-019-02584-3>.
- Lastra, M, Rodil, IF, Sánchez-Mata, A, García-Gallego, M, Mora, J.** 2014. Fate and processing of macroalgal wrack subsidies in beaches of Deception Island, Antarctic Peninsula. *Journal of Sea Research* **88**: 1–10. DOI: <http://dx.doi.org/10.1016/j.seares.2013.12.011>.

- Liebezeit, G, von Bogungen, B.** 1987. Biogenic fluxes in the Bransfield Strait: Planktonic versus macroalgal sources. *Marine Ecology Progress Series* **36**: 23–32.
- Lin, Y, Moreno, C, Marchetti, A, Ducklow, H, Schofield, O, Delage, E, Meredith, M, Li, Z, Eveillard, D, Chaffron, S, Cassar, N.** 2021. Decline in plankton diversity and carbon flux with reduced sea ice extent along the Western Antarctic Peninsula. *Nature Communications* **12**(1): 4948. DOI: <http://dx.doi.org/10.1038/s41467-021-25235-w>.
- Lowe, AT, Galloway, AWE, Yeung, JS, Dethier, MN, Duggins, DO.** 2014. Broad sampling and diverse biomarkers allow characterization of nearshore particulate organic matter. *Oikos* **123**(11): 1341–1354. DOI: <http://dx.doi.org/10.1111/oik.01392>.
- Maksym, T.** 2019. Arctic and Antarctic sea ice change: Contrasts, commonalities, and causes. *Annual Review of Marine Science* **11**(1): 187–213. DOI: <http://dx.doi.org/10.1146/annurev-marine-010816-060610>.
- Matula, CV, Quartino, ML, Nuñez, JD, Zacher, K, Bartsch, I.** 2022. Effects of seawater temperature and seasonal irradiance on growth, reproduction, and survival of the endemic Antarctic brown alga *Desmarestia menziesii* (Phaeophyceae). *Polar Biology* **45**: 559–572. DOI: <http://dx.doi.org/10.1007/s00300-021-02991-5>.
- Meier, WN, Markus, T, Comiso, JC.** 2018. AMSR-E/AMSR2 Unified L3 Daily 12.5 km Brightness Temperatures, Sea Ice Concentration, Motion & Snow Depth Polar Grids, Version 1. [Antarctica]. Boulder, CO: NASA, National Snow and Ice Data Center Distributed Active Archive Center. DOI: <https://doi.org/10.5067/RA1MIJOYPK3P>.
- Meyer, KS, Sweetman, AK.** 2015. Observation of a living macroalga at 166 m in a high Arctic fjord. *Marine Biodiversity Records* **8**: e58. DOI: <http://dx.doi.org/10.1017/S175526721500038X>.
- Michel, LN, Danis, B, Dubois, P, Eleaume, M, Fournier, J, Gallut, C, Jane, P, Lepoint, G.** 2019. Increased sea ice cover alters food web structure in East Antarctica. *Scientific Reports* **9**(1): 8062. DOI: <http://dx.doi.org/10.1038/s41598-019-44605-5>.
- Moe, RL, DeLaca, TE.** 1976. Occurrence of macroscopic algae along the Antarctic Peninsula. *Antarctic Journal of the United States* **11**: 20–24.
- Moran, MD.** 2003. Arguments for rejecting the sequential Bonferroni in ecological studies. *Oikos* **100**(2): 403–405. DOI: <http://dx.doi.org/10.1034/j.1600-0706.2003.12010.x>.
- Morley, SA, Souster, TA, Vause, BJ, Gerrish, L, Peck, LS, Barnes, DKA.** 2022. Benthic biodiversity, carbon storage and the potential for increasing negative feedbacks on climate change in shallow waters of the Antarctic Peninsula. *Biology* **11**(2): 320. DOI: <http://dx.doi.org/10.3390/biology11020320>.
- Mystikou, A, Peters, A, Asensi, A, Fletcher, K, Brickle, P, van West, P, Convey, P, Küpper, F.** 2014. Seaweed biodiversity in the south-western Antarctic Peninsula: Surveying macroalgal community composition in the Adelaide Island/Marguerite Bay region over a 35-year time span. *Polar Biology* **37**(11): 1607–1619. DOI: <http://dx.doi.org/10.1007/s00300-014-1547-1>.
- Nakagawa, S.** 2004. A farewell to Bonferroni: The problems of low statistical power and publication bias. *Behavioral Ecology* **15**(6): 1044–1045. DOI: <http://dx.doi.org/10.1093/beheco/arl107>.
- Neushul, M.** 1965. Diving observation of sub-tidal Antarctic marine vegetation. *Botanica Marina* **8**: 234–243. DOI: <http://dx.doi.org/10.1515/botm.1965.8.2-4.234>.
- Newcombe, EM, Cárdenas, CA.** 2011. Rocky reef benthic assemblages in the Magellan Strait and the South Shetland Islands (Antarctica). *Revista de Biología Marina y Oceanografía* **46**(2): 177–188.
- Nonato, EF, Brito, TAS, De Paiva, PC, Petti, MAV, Corbier, TN.** 2000. Benthic megafauna of the nearshore zone of Martel Inlet (King George Island, South Shetland Islands, Antarctica): Depth zonation and underwater observations. *Polar Biology* **23**(8): 580–588. DOI: <http://dx.doi.org/10.1007/s003000000129>.
- Obryk, MK, Doran, PT, Friedlaender, AS, Gooseff, MN, Li, W, Morgan-Kiss, RM, Priscu, JC, Schofield, O, Stammerjohn, SE, Steinberg, DK, Ducklow, HW.** 2016. Responses of Antarctic marine and freshwater ecosystems to changing ice conditions. *Bioscience* **66**(10): 864–879. DOI: <http://dx.doi.org/10.1093/biosci/biw109>.
- Oliveira, MC, Pellizzari, F, Medeiros, AS, Yokoya, NS.** 2020. Diversity of Antarctic seaweeds, in Gómez, I, Huovinen, P eds., *Antarctic seaweeds: Diversity, adaptation and ecosystem services*. Cham, Switzerland: Springer International Publishing: 23–42.
- Ortega, A, Geraldini, NR, Alam, I, Kamau, AA, Acinas, SG, Logares, R, Gasol, JM, Massana, R, Krause-Jensen, D, Duarte, CM.** 2019. Important contribution of macroalgae to oceanic carbon sequestration. *Nature Geoscience* **12**(9): 748–754. DOI: <http://dx.doi.org/10.1038/s41561-019-0421-8>.
- Pessarrodona, A, Assis, J, Filbee-Dexter, K, Burrows, MT, Gattuso, J-P, Duarte, CM, Krause-Jensen, D, Moore, PJ, Smale, DA, Wernberg, T.** 2022. Global seaweed productivity. *Science Advances* **8**(37): eabn2465. DOI: <http://dx.doi.org/10.1126/sciadv.abn2465>.
- Quartino, M, Boraso de Zaisso, AL, Momo, FR.** 2008. Macroalgal production and the energy cycle of Potter Cove, in Wiencke, C, Ferreira, GA, Abele, D, Marenssi, S eds., *The Antarctic Ecosystem of Potter Cove, King-George Island (Isla 25 de May) Synopsis of Research Performed 1999-2006 at the Dallmann Laboratory and Jubany Station*. Bremerhaven, Germany: Alfred-Wegener Institute: 68–74.
- Quartino, ML, Deregibus, D, Campana, GL, Latorre, GEJ, Momo, FR.** 2013. Evidence of macroalgal colonization on newly ice-free areas following glacial retreat in Potter Cove (South Shetland Islands), Antarctica. *PLoS One* **8**(3): e58223. DOI: <http://dx.doi.org/10.1371/journal.pone.0058223>.

- Quartino, ML, Saravia, LA, Campana, GL, Deregibus, D, Matula, CV, Boraso, AL, Momo, FR.** 2020. Production and biomass of seaweeds in newly ice-free areas: Implications for coastal processes in a changing Antarctic environment, in Gómez, I, Huovinen, P eds., *Antarctic seaweeds: Diversity, adaptation and ecosystem services*. Cham, Switzerland: Springer International Publishing: 155–171.
- Queirós, AM, Stephens, N, Widdicombe, S, Tait, K, McCoy, SJ, Ingels, J, Rühl, S, Airs, R, Beesley, A, Carnovale, G, Cazenave, P, Dashfield, S, Hua, E, Jones, M, Lindeque, P, McNeill, CL, Nunes, J, Parry, H, Pascoe, C, Widdicombe, C, Smyth, T, Atkinson, A, Krause-Jensen, D, Somerfield, PJ.** 2019. Connected macroalgal-sediment systems: Blue carbon and food webs in the deep coastal ocean. *Ecological Monographs* **89**(3): e01366. DOI: <http://dx.doi.org/10.1002/ecm.1366>.
- Rackow, T, Danilov, S, Goessling, HF, Hellmer, HH, Sein, DV, Semmler, T, Sidorenko, D, Jung, T.** 2022. Delayed Antarctic sea-ice decline in high-resolution climate change simulations. *Nature Communications* **13**(1): 637. DOI: <http://dx.doi.org/10.1038/s41467-022-28259-y>.
- Raven, J.** 2018. Blue carbon: Past, present and future, with emphasis on macroalgae. *Biology Letters* **14**(10): 20180336. DOI: <http://dx.doi.org/10.1098/rsbl.2018.0336>.
- Reichardt, W.** 1987. Burial of Antarctic macroalgal debris in bioturbated deep-sea sediments. *Deep-Sea Research* **34**: 1761–1770.
- Reichardt, W, Dieckmann, G.** 1985. Kinetics and trophic role of bacterial degradation of macro-algae in Antarctic coastal waters, in Siegfried, WR, Condy, P, Laws, RM eds., *Antarctic nutrient cycles and food webs*. Berlin, Germany: Springer-Verlag: 115–122.
- Renaud, PE, Løkken, TS, Jørgensen, LL, Berge, J, Johnson, BJ.** 2015. Macroalgal detritus and food-web subsidies along an Arctic fjord depth-gradient. *Frontiers in Marine Science* **2**: 31. DOI: <http://dx.doi.org/10.3389/fmars.2015.00031>.
- Richardson, MG.** 1977. The ecology including physiological aspects of selected Antarctic marine invertebrates associated with inshore macrophytes [PhD dissertation]. Durham, UK: University of Durham, Department of Zoology.
- Roach, LA, Dörr, J, Holmes, CR, Massonnet, F, Blockley, EW, Notz, D, Rackow, T, Raphael, MN, O'Farrell, SP, Bailey, DA, Bitz, CM.** 2020. Antarctic sea ice area in CMIP6. *Geophysical Research Letters* **47**(9): e2019GL086729. DOI: <http://dx.doi.org/10.1029/2019GL086729>.
- Robinson, BJO, Barnes, DKA, Grange, LJ, Morley, SA.** 2021. Intermediate ice scour disturbance is key to maintaining a peak in biodiversity within the shallows of the Western Antarctic Peninsula. *Scientific Reports* **11**(1): 16712. DOI: <http://dx.doi.org/10.1038/s41598-021-96269-9>.
- Robinson, BJO, Morley, SA, Rizouli, A, Sarantopoulou, J, Gkafas, GA, Exadactylos, A, Küpper, FC.** 2022. New confirmed depth limit of Antarctic macroalgae: *Palmaria decipiens* found at 100 m depth in the Southern Ocean. *Polar Biology* **45**(8): 1459–1463. DOI: <http://dx.doi.org/10.1007/s00300-022-03071-y>.
- Sahade, R, Lager, C, Torre, L, Momo, F, Monien, P, Schloss, I, Barnes, DKA, Servetto, N, Tarantelli, S, Tatián, M, Zamboni, N, Abele, D.** 2015. Climate change and glacier retreat drive shifts in an Antarctic benthic ecosystem. *Science Advances* **1**(10): e1500050. DOI: <http://dx.doi.org/10.1126/sciadv.1500050>.
- Säring, F, Veit-Köhler, G, Seifert, D, Liskow, I, Link, H.** 2022. Sea-ice-related environmental drivers affect meiofauna and macrofauna communities differently at large scales (Southern Ocean, Antarctic). *Marine Ecology Progress Series* **700**: 13–37. DOI: <http://dx.doi.org/10.3354/meps14188>.
- Scherrer, KJN, Kortsch, S, Varpe, Ø, Weyhenmeyer, GA, Gulliksen, B, Primicerio, R.** 2019. Mechanistic model identifies increasing light availability due to sea ice reductions as cause for increasing macroalgae cover in the Arctic. *Limnology and Oceanography* **64**(1): 330–341. DOI: <http://dx.doi.org/10.1002/lno.11043>.
- Schimani, K, Zacher, K, Jerosch, K, Pehlke, H, Wiencke, C, Bartsch, I.** 2022. Video survey of deep benthic macroalgae and macroalgal detritus along a glacial Arctic fjord: Kongsfjorden (Spitsbergen). *Polar Biology* **45**(7): 1291–1305. DOI: <http://dx.doi.org/10.1007/s00300-022-03072-x>.
- Smale, D.** 2008. Spatial variability in the distribution of dominant shallow-water benthos at Adelaide Island, Antarctica. *Journal of Experimental Marine Biology and Ecology* **357**(2): 140–148. DOI: <http://dx.doi.org/10.1016/j.jembe.2008.01.014>.
- Smith, CR, DeMaster, DJ, Thomas, C, Sršen, P, Grange, L, Evrard, V, DeLeo, F.** 2012. Pelagic-benthic coupling, food banks, and climate change on the West Antarctic Peninsula shelf. *Oceanography* **25**(3): 188–201.
- Sokal, RR, Rohlf, FJ.** 1995. *Biometry*. New York, NY: W.H. Freeman and Company.
- Stammerjohn, S, Maksym, T.** 2017. Gaining (and losing) Antarctic sea ice: Variability, trends and mechanisms, in Thomas, DN ed., *Sea ice. 3rd ed.* Oxford, UK: Wiley Blackwell: 261–289.
- Tatián, M, Sahade, R, Esnal, GB.** 2004. Diet components in the food of Antarctic ascidians living at low levels of primary production. *Antarctic Science* **16**(3): 123–128. DOI: <http://dx.doi.org/10.1017/S0954102004001890>.
- Tatián, M, Sahade, R, Mercuri, G, Fuentes, V, Antacli, J, Stellfeldt, A, Esnal, G.** 2008. Feeding ecology of benthic filter-feeders at Potter Cove, an Antarctic coastal ecosystem. *Polar Biology* **31**(4): 509–517. DOI: <http://dx.doi.org/10.1007/s00300-007-0379-7>.
- Turner, J, Lu, H, White, I, King, JC, Phillips, T, Hosking, JS, Bracegirdle, TJ, Marshall, GJ, Mulvaney, R, Deb, P.** 2016. Absence of 21st century warming on Antarctic Peninsula consistent with natural variability. *Nature* **535**(7612): 411–415. DOI: <http://dx.doi.org/10.1038/nature18645>.

- Valdivia, N, Díaz, MJ, Holtheuer, J, Garrido, I, Huovinen, P, Gómez, I.** 2014. Up, down, and all around: Scale-dependent spatial variation in rocky-shore communities of Fildes Peninsula, King George Island, Antarctica. *PLoS One* **9**(6): e100714. DOI: <http://dx.doi.org/10.1371/journal.pone.0100714>.
- von Salm, JL, Witowski, CG, Amsler, MO, Amsler, CD, McClintock, JB, Baker, BJ.** 2022. Amphipod diversity and metabolomics of the Antarctic sponge *Dendrilla antarctica*. *Antarctic Science* **34**(5): 349–360. DOI: <http://dx.doi.org/10.1017/S0954102022000268>.
- Wang, M, Liu, X, Jiang, L, Son, S.** 2017. Algorithm Theoretical Basis Document (ATBD): “The VIIRS Ocean Color Products,” Algorithm Theoretical Basis Document Version 1.0. College Park, MD: NOAA NESDIS Center for Satellite Applications and Research.
- White, BA, McClintock, JB, Amsler, CD, Mah, CL, Amsler, MO, White, S, Quetin, LB, Ross, RM.** 2012. The abundance and distribution of echinoderms in near-shore hard-bottom habitats near Anvers Island, western Antarctic Peninsula. *Antarctic Science* **24**(06): 554–560. DOI: <http://dx.doi.org/10.1017/S0954102012000569>.
- Wiencke, C, Amsler, CD.** 2012. Seaweeds and their communities in polar regions, in Wiencke, C, Bischof, K eds., *Seaweed biology: Novel insights into ecophysiology, ecology and utilization*. Berlin, Germany: Springer-Verlag: 265–294.
- Wiencke, C, Amsler, CD, Clayton, MN.** 2014. Macroalgae, in De Broyer, C, Koubbi, P, Griffiths, HJ, Raymond, B, d’Udekem d’Acoz, C, Van de Putte, AP, Danis, B, David, B, Grant, S, Gutt, J, Held, C, Hosie, G, Huetmann, F, Post, A, Ropert-Coudert, Y eds., *Biogeographic Atlas of the Southern Ocean*. Cambridge, UK: Scientific Committee on Antarctic Research: 66–73.
- Wiencke, C, Clayton, MN.** 1990. Sexual reproduction, life history, and early development in culture of the Antarctic brown alga *Himantothallus grandifolius* (Desmarestiales, Phaeophyceae). *Phycologia* **29**(1): 9–18. DOI: <http://dx.doi.org/10.2216/i0031-8884-29-1-9.1>.
- Wiencke, C, Clayton, MN.** 2002. *Antarctic seaweeds. Synopsis of the Antarctic benthos* (vol. 9). Ruggell, Germany: ARG Gantner Verlag, KG.
- Wiencke, C, Clayton, MN, Gómez, I, Iken, K, Lüder, UH, Amsler, CD, Karsten, U, Hanelt, D, Bischof, K, Dunton, K.** 2007. Life strategy, ecophysiology and ecology of seaweeds in polar waters. *Reviews in Environmental Science and Biotechnology* **6**(1): 95–126. DOI: <http://dx.doi.org/10.1007/s11157-006-9106-z>.
- Wiencke, C, Clayton, MN, Langreder, C.** 1996. Life history and seasonal morphogenesis of the endemic Antarctic brown alga *Desmarestia anceps* Montagne. *Botanica Marina* **39**(1–6): 435–444. DOI: <http://dx.doi.org/10.1515/botm.1996.39.1-6.435>.
- Wiencke, C, Clayton, MN, Schulz, D.** 1995. Life history, reproductive morphology and development of the Antarctic brown alga *Desmarestia menziesii* J. Agardh. *Botanica Acta* **108**(3): 201–208. DOI: <http://dx.doi.org/10.1111/j.1438-8677.1995.tb00851.x>.
- Wiencke, C, Stolpe, U, Lehmann, H.** 1991. Morphogenesis of the brown alga *Desmarestia antarctica* cultivated under seasonally fluctuating antarctic daylengths. *Serie Científica INACH* **41**: 65–78.
- Wiktor, JM, Tatarek, A, Kruss, A, Singh, RK, Wiktor, JM, Søreide, JE.** 2022. Comparison of macroalgae meadows in warm Atlantic versus cold Arctic regimes in the high-Arctic Svalbard. *Frontiers in Marine Science* **9**. DOI: <http://dx.doi.org/10.3389/fmars.2022.1021675>.
- Zamorano, JH.** 1983. Zonación y biomasa de la macrofauna bentónica en Bahía South, Archipiélago de Palmer, Antártica. *Serie Científica INACH* **30**: 27–38.
- Zaneveld, JS.** 1966. The occurrence of benthic marine algae under shore fast-ice in the western Ross Sea, Antarctica. *Proceedings of the International Seaweed Symposium* **5**: 217–231.
- Zar, JH.** 1984. *Biostatistical analysis. 2nd ed.* Englewood Cliffs, NJ: Prentice-Hall.
- Zieliński, K.** 1990. Bottom macroalgae of the Admiralty Bay (King George Island, South Shetlands, Antarctica). *Polish Polar Research* **11**: 95–131.
- Zwerschke, N, Morley, SA, Peck, LS, Barnes, DKA.** 2021. Can Antarctica’s shallow zoobenthos “bounce back” from iceberg scouring impacts driven by climate change? *Global Change Biology* **27**(13): 3157–3165. DOI: <http://dx.doi.org/10.1111/gcb.15617>.

How to cite this article: Amsler, CD, Amsler, MO, Klein, AG, Galloway, AWE, Iken, K, McClintock, JB, Heiser, S, Lowe, AT, Schram, JB, Whippo, R. 2023. Strong correlations of sea ice cover with macroalgal cover along the Antarctic Peninsula: Ramifications for present and future benthic communities. *Elementa: Science of the Anthropocene* 11(1). DOI: <https://doi.org/10.1525/elementa.2023.00020>

Domain Editor-in-Chief: Jody W. Deming, University of Washington, Seattle, WA, USA

Associate Editor: Kevin R. Arrigo, Environmental Earth System Science, Stanford University, Stanford, CA, USA

Knowledge Domain: Ocean Science

Published: June 30, 2023 **Accepted:** May 17, 2023 **Submitted:** January 17, 2023

Copyright: © 2023 The Author(s). This is an open-access article distributed under the terms of the Creative Commons Attribution 4.0 International License (CC-BY 4.0), which permits unrestricted use, distribution, and reproduction in any medium, provided the original author and source are credited. See <http://creativecommons.org/licenses/by/4.0/>.



Elem Sci Anth is a peer-reviewed open access journal published by University of California Press.

OPEN ACCESS The Open Access icon, which is a stylized padlock with a circular arrow around it, indicating that the content is freely available.